Received: 16 May 2021 | Revised: 15 June 2021 | Accepted: 18 June 2021

DOI: 10.1002/aoc.6353

RESEARCH ARTICLE

Applied Organometallic Chemistry WILEY

Octa-substituted Zinc(II), Cu(II), and Co(II) phthalocyanines with 1-(4-hydroxyphenyl)propane-1-one: Synthesis, sensitive protonation behaviors, Ag(I) induced H-type aggregation properties, antibacterial–antioxidant activity, and molecular docking studies

Ahmet T. Bilgiçli[1] | **Tugberk Kandemir**[1] | **Burak Tüzün**[2] | **Rana Arıduru**[1] | **Armağan Günsel**[1] | **Çağla Abak**[1] | **M. Nilüfer Yarasir**[1] | **Gulnur Arabaci**[1]

[1]Department of Chemistry, Sakarya University, Sakarya, Turkey

[2]Department of Chemistry, Cumhuriyet University, Sivas, Turkey

Correspondence
Ahmet T. Bilgiçli, PhD, Department of Chemistry, Sakarya University, 54140, Esentepe, Sakarya, Turkey.
Email: abilgicli@sakarya.edu.tr

Gulnur Arabaci, Department of Chemistry, Sakarya University, Sakarya, Turkey.
Email: garabaci@sakarya.edu.tr

Funding information
Scientific and Technological Research Council of Turkey, Grant/Award Number: 116Z052

Abstract

This study shows the synthesis and characterization of 4,5-bis(4-propionylphenoxy)phthalonitrile (**2**) and its octa-substituted phthalocyanine derivatives [ZnPc(**3**), CuPc(**4**), and CoPc(**5**)]. A combination of standard spectroscopic techniques has characterized the newly synthesized phthalonitrile derivative and phthalocyanines. The aggregation behaviors of new octa-substituted phthalocyanines have been evaluated by ultraviolet–visible (UV-vis) spectroscopy. The metal ion-sensitive behaviors of new octa-substituted phthalocyanines in the presence of soft metal ions have been performed by UV-vis and fluorescence spectrophotometer. The quenching efficiency (K_{sv}) of Ag^{+} ions against ZnPc(**3**) was found using the Stern–Volmer equation. The binding constant (K_a) and binding stoichiometry (n) of ZnPc(**3**) with Ag^{+} ions were calculated using the modified Benesi–Hildebrand equation. Sensitive protonation behaviors of octa-substituted phthalocyanines have been investigated by titration experiments as well as computational calculations. The ZnPc(**3**) and CuPc(**4**) were exhibited H-type aggregation behaviors toward Ag^{+} ions. However, the protonation of octa-substituted zinc and copper phthalocyanine during the titration with HCl caused J-type self-aggregation properties. In vitro antioxidant properties of the new compounds were investigated by the radical scavenging ability of 1,1-diphenyl-2-picrylhydrazyl (DPPH), chelating ability to ferrous ions, and reducing power methods. Additionally, in vitro antibacterial activities of the octa-substituted phthalocyanines were determined. Finally, optimized structures of novel compounds [(**2**), ZnPc(**3**), CuPc(**4**), and CoPc(**5**)] were obtained on the HF (Hartree–Fock), B3LYP (Becke, 3-parameter, Lee-Yang-Parr), M06–2X methods with 3–21 g, 6–31 g and SDD basis set. Then, biological activities of

novel phthalonitrile and its phthalocyanine derivatives toward breast, liver, and lung cancer proteins were compared with molecular docking studies.

KEYWORDS

antimicrobial and antioxidant, H- or J-type aggregation, molecular docking, phthalocyanine, protonation

1 | INTRODUCTION

Metals that function in the cellular and subcellular systems of living organisms are as crucial as organic molecules for the life process. Because some of these metals are in the structure of inorganic salts in living systems, studies on metal-containing compounds are gaining momentum with increasing interest on the grounds that they will contribute to a better understanding of biochemical systems. The use of metals as antibacterial agents such as antibiotics dates back thousands of years.[1] However, as bacteria gained resistance to existing antibiotics, it became essential to research and synthesize new compounds with the potential to become drugs. The primary purpose of antibacterial agents is to show high efficacy in low doses and without resistance development. Unlike traditional antibacterial agents, metals are regaining interest as antibacterial and biocidal agents, as they target multiple cellular processes that cause pleiotropic effects on bacterial cells.[2,3] Metal-containing organic compounds have larger three-dimensional geometries compared with pure organic compounds. These properties make them a good starting point for discovering and researching new drugs. The results of studying metal-containing compounds have played a seminal role in medicinal chemistry in recent years. In particular, the discovery of the anticancer drug cisplatin and its use in most cancer treatments today can be considered the real beginning of inorganic medical chemistry. After this discovery, research on metal-containing organic compounds gained more importance.[4,5] One group of the most promising molecules in this field are phthalocyanine compounds that can mimic the properties of biologically important molecules such as chlorophyll and hemoglobin.[6,7] It is also well known that various metals are toxic to bacteria and the d-block transition metals are the most toxic among them.[7] Therefore, it is crucial to synthesize phthalocyanines with d-block metals and determine their antibacterial and antioxidant properties. Thus, studies on the synthesis of phthalocyanine derivatives and investigation of their antioxidant and antibacterial properties have also increased in recent years.[8–11]

Antioxidants are substances that help neutralize or reduce the free radicals, which are waste materials produced by cells against stress. Free radicals are also known as reactive oxygen species (ROS) caused by internal effects, such as inflammation, or external influences, such as pollution, UV-light exposure, and cigarette smoke. The free radicals or ROS can play essential roles in developing serious chronic diseases, including cardiovascular diseases, aging, heart disease, and cancer.[12] Antioxidants, divided into two main groups as synthetic and natural, are used in food, cosmetics, and pharmacy. Therefore, researchers are interested in synthesizing and developing new molecules as it leads to the conclusion that new antioxidant molecules can also be applied in new industries. In this context, phthalocyanines are the leading substances. The synthesis of different types of these molecules with their various biological properties has gained importance among scientists.[12,13]

Phthalocyanines, known as tetrabenzo[5,10,14,15] tetraazaporphyrin, have thermally and chemically stable structures owing to their conjugated 18 π-electron systems. Due to their stable structures with having high extinction coefficients ($\varepsilon_{max} > 1.0 \times 10^5$ M^{-1} cm^{-1}) and long absorption wavelength maxima (600 nm > λ_{max} > 900 nm), they have promising applications in many fields from chemical sensors to solar cells, from nonlinear optics to photodynamic therapy.[14–19] However, the tendency of unsubstituted phthalocyanines to self-assemble causes limitations in determining their superior properties. It is well known that the aggregation tendency of phthalocyanines has a negative effect on their optical properties in addition to causing low solubility. Therefore, in addition to increasing their solubility, control of their aggregation is of primary importance in phthalocyanine chemistry. Phthalocyanines generally form H-type aggregates in solution. This is due to the regularity of push and pull forces in H-aggregation. Because of the 18-π electrons conjugated by π–π and Van der Waals interactions, the molecules overlap strongly and tend to form columnar stacks. Besides, concentration, temperature, nature of the substituents, nature of the solvent and additives, and the metal ion in the

center are effective factors on aggregation.[20,21] J-type aggregates are less common in phthalocyanine complexes than H-type aggregates and usually occur by metal–ligand interaction.[22] It is well known that the substitution of bulky groups in the peripheral/nonperipheral positions of phthalocyanines increases their solubility in common organic solvents. Phthalocyanines containing 1-(4-hydroxyphenyl) propane-1-one groups previously synthesized by our group have been found to have very high solubility in many organic solvents such as $CHCl_3$, CH_2Cl_2, THF, toluene, DMF, and DMSO,[23,24] and within the scope of this study, it was found that the electronic spectra of novel octa-substituted phthalocyanine derivatives bearing 1-(4-hydroxyphenyl)propane-1-one are highly dependent on acid concentration. The green color of phthalocyanines was changed to pale green in the presence of HCl, which can be observed even with the naked eye.

Theoretical calculations are becoming more popular every day. It is seen that the results obtained by many theoretical calculations are in significant agreement with the experimental results.[25,26] Recently, theoretical methods are used to compare the chemical and biological activities of novel drug compounds. In this method, the drug compound's chemical and biological activities are predicted from the numerical values of the parameters obtained thanks to density functional theory (DFT) calculations. Also, molecular docking calculations are commonly used to get some information about biological activities. Some proteins used in these calculations are the crystal structure of the BRCT repeat region from the breast cancer-associated protein, ID: 1JNX,[27] the crystal structure of lung cancer protein, ID: 5ZMA,[28] and the crystal structure of the deleted in Liver Cancer 2 (DLC2), ID: 2H80.[29]

In this study, new phthalonitrile derivative, 4,5-bis (4-propionylphenoxy)phthalonitrile and its new octa-substituted phthalocyanine derivatives [ZnPc(**3**), CuPc(**4**), and CoPc(**5**)] have been synthesized. The new compounds have been characterized by a combination of various spectroscopic techniques such as FT-IR, ^{1}H-NMR, ^{13}C-NMR, MALDI-TOF, UV-vis, and fluorescence spectroscopy. We also were presented aggregation behaviors of new octa-substituted phthalocyanines at different concentrations. Metal-induced aggregation behaviors of new phthalocyanines have been evaluated by UV-vis and fluorescence spectroscopy. Sensitive protonation behaviors of octa-substituted phthalocyanines have been investigated by titration experiments as well as computational calculations. Additionally, the antioxidant and antibacterial properties of the new octa-substituted phthalocyanine derivatives were examined, and the results were interpreted. Finally, biological activities of novel compounds [(**2**), ZnPc(**3**), CuPc(**4**), and CoPc(**5**)] were evaluated by molecular docking studies.

2 | EXPERIMENTAL

2.1 | Materials and apparatus

The chemical compounds used in reactions were obtained from commercial companies (Merck, Sigma-Aldrich, and Fluka). The purchased chemical compounds were used without further purification. FT-IR spectra of synthesized compounds were recorded by the Perkin Elmer Spectrum Two FT-IR (ATR sampling accessory) spectrometer. ^{1}H- and ^{13}C-NMR spectra were taken using a Varian 300-MHz Mercury Plus instrument using TMS as internal standards. The mass spectra of novel compounds were acquired on a Bruker Microflex LT MALDI-TOF MS. UV-vis spectra of new octa-substituted phthalocyanine derivatives were recorded by Agilent Model 8453 diode array UV-vis spectrophotometer. Fluorescence measurements were achieved by the Hitachi S-7000 fluorescence spectrophotometer.

2.2 | Syntheses

2.2.1 | The synthesis of 4,5-bis (4-propionylphenoxy)phthalonitrile (**2**)

1-(4-hydroxyphenyl)propane-1-one (1.52 g, 10.13 mmol) dissolved in 40-ml THF was a mixture with anhydrous K_2CO_3 (7.0 g, 50.72 mmol) for 20 min at 60°C. Then, 4,5-dichloro-1,2-dicyanobenzene solution dissolved in 30-ml THF (1.0 g, 5.07 mmol) was added to the reaction mixture drop by drop within 30 min. The obtained mixture was efficiently stirred 24 h at reflux temperature. After the completion of the reaction, it was cooled to room temperature (≈25°C) and filtered. The solid product was obtained by removing the solvent by an evaporation method. The solid product was washed with n-hexane several times and crystallized using ethanol.

Yield of compound (**2**): 1.21 g (56%). Anal. Calcd. for $C_{26}H_{20}N_2O_4$ (424.45 g/mol): C, 73.57; H, 4.75; N, 6.60. Found: C, 73.21; H, 4.65; N, 6.68. FT-IR (υ_{max}/cm^{-1}): 3075, 3055, 3020, 2963, 2929, 2896, 2868, 1652, 1595, 1560 1370, 1338, 1212, 1156, 1004, 847, 786, 591. ^{1}H NMR (300 MHz, DMSO-d6) δ 7.90–7.72 (d, 4H), 7.10 (s, 2H), 6.90–6.62 (m, 4H), 2.89 (q, 4H), 1.03 (m, 6H). ^{13}C-NMR (75 MHz, DMSO) δ 199.29(2C), 162.78(2C), 138.22(2C), 136.20(2C), 130.98(4C), 128.69(2C), 119.12(2C), 115.88 (4C), 115.21(2C), 31.26(2C), 9.09(2C). Mass: m/z: 429.238 $[M + 3H]^+$.

2.2.2 | General procedure for the synthesis of phthalocyanines [ZnPc(**3**), CuPc(**4**), and CoPc(**5**)]

Anhydrous related metal salts (zinc acetate or copper chloride or cobalt chloride) and 0.10 g 4,5-bis(4-propionylphenoxy)phthalonitrile (**2**) were heated at 140°C in *N*,*N*-dimethylaminoethanol/DBU media. The reaction was continued for 8 h. After the completion of the reaction, obtained green product was precipitated with MeOH and filtered off. They were washed with n-hexane and MeOH several times. Further purification of new octa-substituted phthalocyanine derivatives was achieved by column chromatography using dichloromethane/THF (50:5 v/v) as the eluent.

2,3,9,10,16,17,23,24-octacis(1-(4-hydroxyphenyl)propan-1-one)phthalocyaninato zinc(II)

Yield of compound (**3**): 36 mg (35%). Chemical Formula: $C_{103}H_{78}N_8O_{16}Zn$ (Molecular Weight: 1749.18 g/mol), Elemental Analysis: Calculated: C, 70.72; H, 4.49; N, 6.41; Found: C, 71.02; H, 4.56; N, 6.34. FT-IR (υ_{max}/cm^{-1}): 3098, 3,061 (Ar-CH), 2975, 2940, 2864 (Alip-CH), 1683(C═O), 1600, 1502, 1446, 1389, 1355, 1271, 1215, 1166 (Ar–O–Ar), 1082, 1013, 992, 949, 897, 838, 796, 566. ^{1}H NMR (300 MHz, DMSO-d6) δ 8.20–7.68 (m), 7.31(s), 7.02–6.68 (m), 2.96 (q), 0.98 (m). UV-vis (λ_{max}, nm, in THF): 674 (Q-band), 613 (Vibrational satellite) 353 (B-band). MS (MALDI-MS, 2,5-dihydroxybenzoic acid as matrix): 1798.178 $[M + 2Na + 2H]^+$.

2,3,9,10,16,17,23,24-octacis(1-(4-hydroxyphenyl)propan-1-one)phthalocyaninato copper(II)

Yield of compound (**4**): 33 mg (32%). Chemical Formula: $C_{103}H_{78}CuN_8O_{16}$ (Molecular Weight: 1747.31 g/mol), Elemental Analysis: Calculated: C, 70.80; H, 4.50; N, 6.41; Found: C, 71.14; H, 4.45; N, 6.68. FT-IR (υ_{max}/cm^{-1}): 3061 (Ar-CH), 2974, 2932, 2874 (Alip-CH), 1682 (C═O), 1592, 1501, 1439, 1403, 1348, 1270, 1250, 1208, 1159 (Ar–O–Ar), 1096, 1005, 949, 894, 844, 796, 747, 607, 559. UV-vis (λ_{max}, nm, in THF): nm 676 (Q-band), 615 (Vibrational satellite) 355 (B-band). MS (MALDI-MS, 2,5-dihydroxybenzoic acid as matrix): 1770.132 $[M + Na + H]^+$.

2,3,9,10,16,17,23,24-octacis(1-(4-hydroxyphenyl)propan-1-one)phthalocyaninato cobalt(II)

Yield of compound (**5**): 29 g (28%). Chemical Formula: $C_{103}H_{78}CoN_8O_{16}$ (Molecular Weight: 1742.70 g/mol), Elemental Analysis: Calculated: C, 70.99; H, 4.51; N, 6.43; Found: C, 71.36; H, 4.72; N, 6.39. FT-IR (υ_{max}/cm^{-1}): 3098, 3,061 (Ar-CH), 2975, 2933, 2905, 2877 (Alip-CH), 1682 (C═O), 1592, 1502, 1453, 1403, 1348, 1271, 1250, 1215, 1160 (Ar–O–Ar), 1096, 1006, 949, 901, 845, 796, 748, 559. UV-vis (λ_{max}, nm, in THF): 660 (Q-band), 601 (Vibrational satellite) 333 (B-band). MS (MALDI-MS, 2,5-dihydroxybenzoic acid as matrix): 1746.317 $[M + 3H]^+$, 1832.008 $[M + 2Na + K + 2H]^+$.

2.3 | Fluorescence measurement

Fluorescence properties of phthalocyanine derivative with zinc metal in its center were determined in THF solution at room temperature (≈25°C). Fluorescence quantum yields (Φ_F) were calculated by Equation 1.[30,31]

$$\Phi_F = \Phi_F(\text{Std})\ \frac{A_{Std}\cdot F\cdot n^2}{A\cdot F_{Std}\cdot n_{std}^2}. \quad (1)$$

In this equation, Φ_F is the quantum yields of the novel synthesized compounds, Φ_F (Std) is the quantum yield of the reference compound, F and F_{Std} are the areas under the fluorescence emission curves of ZnPc(**3**) and unsubstituted zinc phthalocyanine as a standard, respectively. A_{Std} and A are the absorbance of unsubstituted zinc phthalocyanine and ZnPc(**3**), respectively. n^2 and n_{Std}^2 are the refractive indices of used solvents. The quantum yield of unsubstituted zinc phthalocyanine was used as 0.23.[32]

The quenching efficiency (K_{sv}) of Ag(I) ions against octa-substituted zinc phthalocyanine were found using the Stern–Volmer equation (Equation 2). The binding constant (K_a) and binding stoichiometry (n) of ZnPc(**3**) with Ag(I) ions were calculated using the modified Benesi–Hildebrand equation (Equation 3).

$$F_0/F = 1 + K_{sv}[M^{z+}], \quad (2)$$

$$\log[(F_0 - F)/F] = \log K_a + n\cdot\log[M^{z+}]. \quad (3)$$

In Equations 2 and 3, "F_0" and "F" are fluorescence intensity of ZnPc(**3**) in the absence and presence of Ag(I) ions, respectively. "K_{sv}" is the Stern–Volmer quenching constant, $[M^{z+}]$ is the concentration of Ag^+ ions, "K_a" is the binding constant, and "n" is binding stoichiometry.[33]

2.4 | Determinations of antioxidant activities

2.4.1 | DPPH radical scavenging activity

1,1-diphenyl-2-picrylhydrazyl (DPPH) radical scavenging activity was tested using the method of Blois[34]; 2 ml of

methanol solution of DPPH (0.004%) was mixed to 500 µl of Pc compound (with and without metal) solutions at different concentrations from 100 to 500 µg ml^{-1}). The mixture was vigorously vortexed and kept in the dark for 30 min at room temperature. After that, the mixture absorbance was monitored at 517 nm using a UV-vis spectrophotometer. The control experiment was performed in the same way as the reaction experiment without phthalocyanine compound. DPPH radical scavenging activity was calculated by the following equation (Equation 4):

$$\text{DPPH scavenging activity}\,(\%) = 1 - \left(A_{\text{sample517}}/A_{\text{control517}}\right) \times 100, \quad (4)$$

where $A_{\text{control517}}$ is the absorbance of the control (containing all reagents except the tested Pc) and $A_{\text{sample517}}$ is the absorbance in the presence of Pc compound or standards. Trolox and BHT were selected to use as standards, and their scavenging activities were evaluated with the results of phthalocyanine compounds. All experiments were repeated three times, and the data achieved were the arithmetic mean of three measurements.

2.4.2 | Determination of metal chelating activity on ferrous ions

The study of ferrous ion chelating activities for the synthesized Pc compounds was performed according to the method described in the Dinis et al. work.[35] Briefly, 1 ml of sample solution at different concentrations of Pc compound (100–500 µg ml^{-1}) was mixed with 0.1 ml of $FeCl_2$ (2 mM), and 3.7 ml of distilled water in a test tube. The mixture solution was vortexed and incubated at room temperature for 30 min. After the time was complete, 0.2 ml of 5-mM ferrosine solution was mixed into the test tube and incubated at room temperature for a further 10 min. The absorption of the solution was then observed spectrophotometrically at 562 nm. The control reaction was performed by a solution containing only $FeCl_2$ and ferrosine substances. The percentage of inhibition of ferrozine-Fe^{2+} complex formation was calculated using the equation given below (Equation 5):

$$\text{Ferrous ion chelating activity}\,(\%) = 1 - \left(A_{\text{S562}}/A_{\text{C562}}\right) \times 100, \quad (5)$$

where A_{C562} was the absorbance of the control and A_{S562} is the absorbance in the presence of Pc compound or standard. Ethylenediaminetetraacetic acid (EDTA) was preferably used as the standard, and results obtained for novel octa-substituted phthalocyanine compounds were compared with the standard. All experiments were repeated three times, and the data achieved were the arithmetic mean of three measurements.

2.4.3 | Reducing power activity

The reducing power activities of Pc compounds were studied as reported by Oyaizu[36]; 2.5 ml of Pc compound solution at different concentrations (5–100 µg ml^{-1}) was mixed with 2.5 ml of the buffer (0.2-M phosphate buffer at pH 6.6) and 2.5 ml of potassium ferricyanide [$K_3Fe(CN)_6$] (1%) and incubated at 50°C for 20 min. After the incubation was completed, 2.5 ml of trichloroacetic acid (10%) was supplemented to the reaction mixture to stop the reaction. The reaction mixture was centrifuged at 2500 rpm for 10 min. Then, 2.5 ml of the supernatant was taken and mixed with 0.5 ml of $FeCl_3$ (0.1%) and 2.5 ml of distilled water, and the absorption of the reaction was monitored at 700 nm. Ascorbic acid, BHT, and Trolox were used as positive standards. Increasing absorption values of the reaction mixture have identified increasing the reducing power.

2.5 | Determination of antibacterial activity

In vitro antibacterial activities of the synthesized phthalocyanine compounds were screened by using the agar well diffusion method.[37] The antibacterial activities were determined against *Escherichia coli* (ATCC 25922) as a gram-negative bacteriuum and *Staphylococcus aureus* (ATCC 25923), *Bacillus cereus* (SBT8) as gram-positive bacteria. Each bacterial strain was swabbed uniformly onto individual Mueller Hinton agar plates. In each plate, wells were cut out using a standard cork borer (6-mm diameter); 20 µl of the compound solution was added to each well. After incubation at 37°C for 24 h, the diameter of inhibition zones was measured in millimeter, and the results were recorded. DMSO was used as a solvent and was run with the experiment under the same condition as a negative control. While, ampicillin (AMP, 10 µg) disc was used as a positive control for comparison. The results were represented in Table 1.

2.6 | Theoretical calculations

It has been observed that theoretical studies have become widespread and developed in recent studies. GaussView 5.0.8,[38] ChemDraw Professional 15.1,[39] Gaussian09 AS64L-G09RevD.01,[40] and Chemcraft V1.8[41] package programs were used in the calculations within scopes of this study. Many quantum chemical parameters of 4,5-bis(4-propionylphenoxy)phthalonitrile (**2**) and its

TABLE 1 Spectral parameters and photophysical properties (Φ_F) of novel synthesized phthalocyanines [ZnPc(**3**), CuPc(**4**), and CoPc(**5**)] in THF

	Absorbance			Fluorescence			
Compounds	λ_{max}^{abs} (nm) **(Q-band)**	λ_{max}^{abs} (nm) **(B-band)**	λ_{max}^{abs} (nm) **(Vibrational satellite)**	$\lambda_{max}^{em.}$ (nm) **(emission)**	$\lambda_{max}^{exc.}$ (nm) **(excitation)**	**Δλ (nm) (Stokes shift)**	**Φ_F, % (quantum yield)**
3	674	353	613	690	673	17	0.12
4	676	355	615	-	-	-	-
5	660	333	601	-	-	-	-
ZnPc[a]	666[a]	342[a]	-	673[a]	666[a]	7[a]	0.23[a]

[a]From Saka et al.[32]

octa-substituted phthalocyanine derivatives [ZnPc(**3**), CuPc(**4**), and CoPc(**5**)] were found with the help of these programs. Chemical activity values of phthalonitrile (**2**) and its phthalocyanine derivatives (**3–5**) were performed by the Hartree–Fock (HF) method,[42] Becke, three-parameter, Lee-Yang-Parr (B3LYP),[43] and M06-2X[44] method with 6-31G basis set. The activities of the molecules were compared with the help of these parameters. Many parameters have been calculated such as E_{HOMO} (highest occupied molecular orbital), E_{LUMO} (lowest unoccupied molecular orbital), ΔE (HOMO − LUMO) energy gap, chemical hardness (η), chemical potential (μ), nucleophilicity (ε), electronegativity (χ), electrophilicity (ω), global softness (σ), and proton affinity (PA).[45,46] With the help of these parameters, comments on their chemical activities were made.

Apart from DFT calculations, molecular docking calculations were used to compare the biological activities of compound (**2**) and its metal complexes (**3–5**). Proteins used in molecular docking calculations were taken from the protein data bank site and used the HEX 8.0.0 program.[47] In this calculation, some important parameters are as follows: correlation type (shape only), FFT mode (3D), grid dimension (0.6), receptor range (180), ligand range (180), twist range (360), and distance range (40). Also, protein–ligand interaction profiler (PLIP) server was used to examine the interaction between protein and phthalonitrile (**1**) and its metal complexes (**3–5**).[48]

3 | RESULT AND DISCUSSION

3.1 | Synthesis and characterization

The precursor dinitrile derivative, 4,5-dichlorophthalonitrile, was carried out according to the literature.[49] The new phthalonitrile derivative, 4,5-bis(4-propionylphenoxy) phthalonitrile (**2**), was synthesized by aromatic nucleophilic substitution reaction between 4,5-dichlorophthalonitrile and 1-(4-hydroxyphenyl) propane-1-one (Scheme 1). The new octa-substituted phthalocyanine derivatives [ZnPc(**3**), CuPc(**4**), and CoPc (**5**)] were achieved by cyclotetramerization reaction in the presence of zinc acetate or copper chloride or cobalt chloride salts in *N*,*N*-dimethylaminoethanol/DBU media (Scheme 2). The octa-substituted phthalocyanine derivatives are not soluble in hexane, EtOH, and MeOH. Therefore, they were washed with these solvents several times to remove impurities. For further purification, chromatography on the silica-gel column was used. The structures of target phthalonitrile and its octa-substituted phthalocyanine derivatives were characterized by using general spectroscopic techniques such as FT-IR, ^{1}H-NMR, MS, UV-vis spectroscopy, and fluorescence spectroscopy.

Infrared spectroscopy is widely used mainly for the detection of functional groups. For this reason, the structures of the newly synthesized phthalonitrile derivative and its phthalocyanine derivatives were characterized by FTIR spectra. In Cl-bonded benzene derivatives, the C–Cl stretching frequency is usually observed in the 900- to 500-cm^{-1} region, depending on the configuration and conformation of the compound.[50] Planar C–Cl strains of 4,5-dichlorophthalonitrile, the precursor phthalonitrile derivative, of about 917, 679, and 525 cm^{-1} were observed. Polar C–Cl bonds are weaker than C–H bonds and more prone to attack by a nucleophile. It can rapidly replace with nucleophiles.[51] After the displacement reaction was completed, peaks of C-CI vibrations were not observed in the newly synthesized compound 4,5-bis (4-propionylphenoxy)phthalonitrile (**2**). This shows that the Cl atoms are abstracted due to displacement reaction. Also, the characteristic C≡N peak at 2239 cm^{-1} for 4,5-dichlorophthalonitrile shifted to 2227 cm^{-1}. The newly synthesized compound (**2**) has characteristic peaks

SCHEME 1 The synthesis of 4,5-bis (4-propionylphenoxy)phthalonitrile (**2**) (THF, K_2CO_3, 65°C, 24 h)

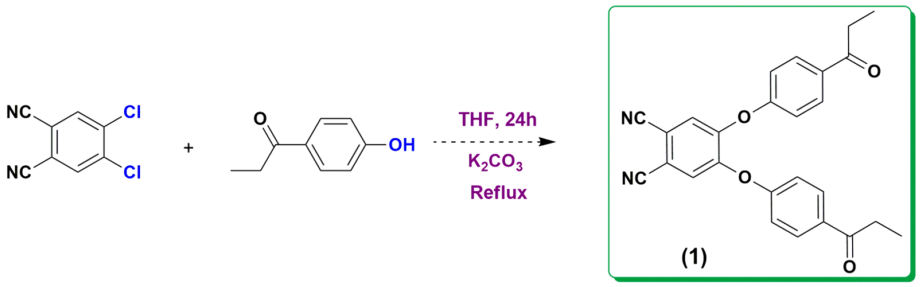

SCHEME 2 The synthesis of new phthalocyanine derivatives [ZnPc(**3**), CuPc(**4**), and CoPc(**5**)] (*N*,*N*-dimethylaminoethanol/ DBU, 140°C, 8 h)

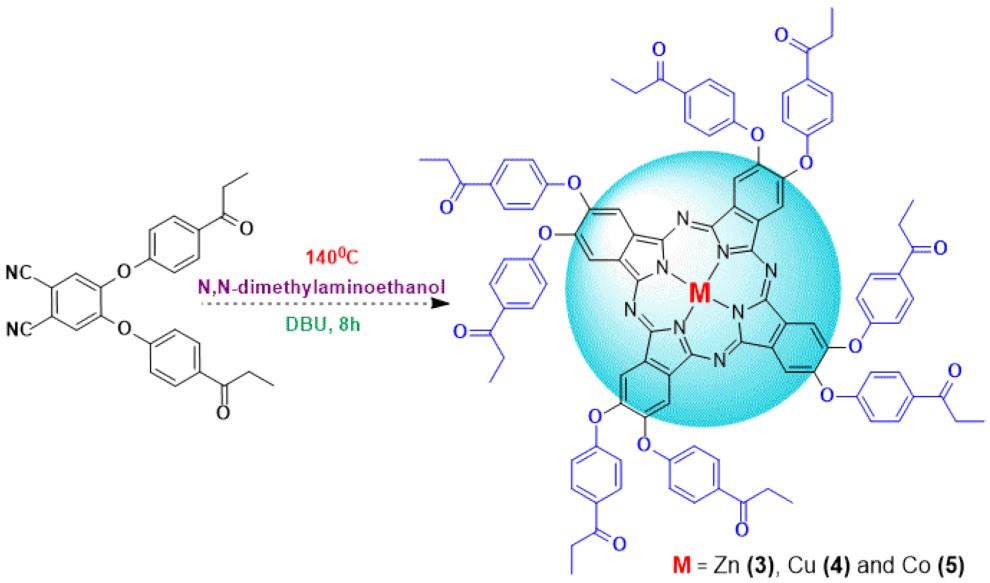

such as Aromatic-CH, Aliphatic-CH, –C≡N, C═O (carbonyl), and Ar–O–Ar stretches in FTIR spectra. They appeared at 3075, 3055, 3020, 2963, 2929, 2896, 2868, 1652, 1212, and 1156 cm^{-1}, respectively (Figure S1).

In the FTIR spectra taken after the synthesis of phthalocyanine derivatives [ZnPc(**3**), CuPc(**4**), and CoPc(**5**)], the characteristic C≡N peak belonging to the phthalonitrile derivative (**2**) at 2227 cm^{-1} disappeared. This may be evidence that the cyclotetramerization reaction has occurred. In the FTIR spectra of the phthalocyanine derivatives, very similar spectra were obtained except for small shifts. As expected, Ar-CH peaks occurred between 3200 and 3000 cm^{-1} and Alip-CH peaks between 3000 and 2800cm^{-1}. The Ar–O–Ar peak has been recorded as severe peaks around 1200–1100cm^{-1} (Figure S2 for ZnPc(**3**), Figure S3 for CuPc(**4**), and Figure S4 for CoPc(**5**)).

The structures of the synthesized new compounds were tried to be elucidated by NMR spectroscopy. ^{1}H-NMR and ^{13}C-NMR spectra of synthesized new compounds were obtained in deuterated dimethyl sulphoxide (d6-DMSO) solution (Figures S5 and S6). In the ^{1}H-NMR spectrum of 4,5-bis (4propionylphenoxy) phthalonitrile (**2**), aromatic protons ortho to C≡N groups appeared as a single peak at 7.1 ppm. Aromatic peaks of the substituted group were obtained as a doublet at 6.79 and 7.80 ppm. Aliphatic protons in the substituted group were observed at 2.89 and 1.03 ppm. ^{13}C-NMR spectrum confirmed the structure of the new phthalonitrile derivative. Carbon peak belonging to the keto group was observed at 199.29 ppm, carbon atoms of the benzene ring between 162.78 and 128.69 ppm, nitrile carbons at 115.88 ppm, aliphatic peaks at 31.26 and 9.09 ppm. The ^{1}H-NMR spectrum of ZnPc(**3**) showed expected signals. But aromatic protons were observed as broad peaks due to the aggregation of phthalocyanines in high concentrations. ^{1}H-NMR spectra of CuPc(**4**) and CoPc(**5**) could not be recorded due to paramagnetic properties.[52]

The MALDI-TOF mass spectrometry technique also confirmed the newly synthesized 4,5-bis(4-propionylphenoxy)phthalonitrile and its octa-substituted phthalocyanine derivatives structures. The protonated ion peak of compound (**2**) was observed in the mass spectrum (Figure S7). The MALDI-TOF spectra of new octa-substituted phthalocyanine derivatives [ZnPc(**3**), CuPc(**4**), and CoPc(**5**)] were observed as sodium added peaks. This indicates that sodium selectivity of octa-substituted phthalocyanine derivatives was high

(Figure S8 for ZnPc(**3**), Figure S9 for CuPc(**4**), and Figure S10 for CoPc(**5**)).

3.2 | Electronic absorption spectra of new octa-substituted phthalocyanines

UV-vis spectroscopy is the most widely used technique in the characterization of phthalocyanine compounds as it provides more meaningful information than other spectroscopic techniques. Because phthalocyanines are rich in π-electron, they give different absorption bands in the UV-vis spectrum. These peaks are the result of π–π* and deeper π–π* transitions.[15] These are Q-bands occurring between 720 and 500 nm and B or Soret bands seen between 420 and 285 nm, and in some molecules, charge transfer transitions caused by metal–ligand, ligand–metal transitions can also be observed.

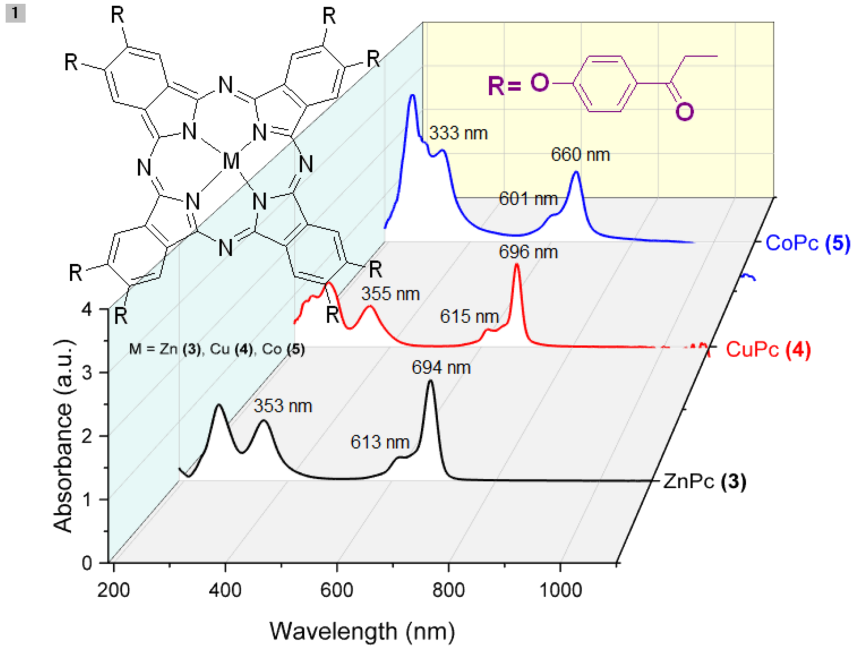

FIGURE 1 UV-vis spectra of new phthalocyanine derivatives [ZnPc(**3**), CuPc(**4**), and CoPc(**5**)] in THF

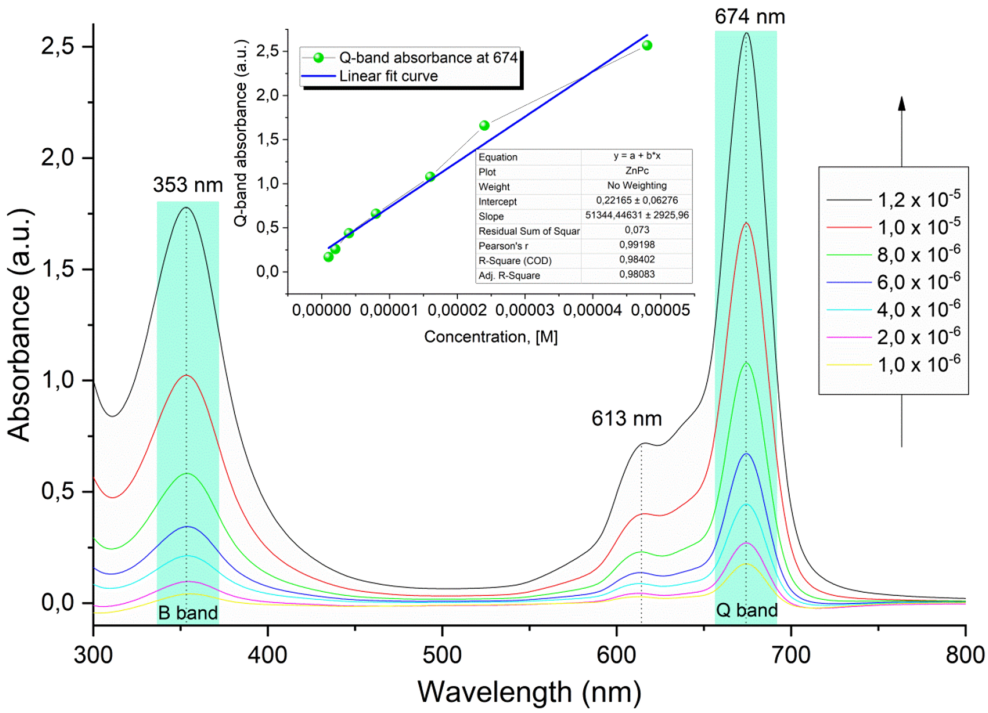

FIGURE 2 Electronic spectra of ZnPc(**3**) at different concentration values (inset: the plot of Q-band absorbance versus concentration)

Characteristic Q-bands of phthalocyanine compounds help us understand whether the phthalocyanine compounds are metallic or metal-free. In the electronic spectra of metal phthalocyanines, Q-bands appear as a single band. In contrast, in metal-free phthalocyanines, the Q-band is obtained as split in two due to molecular symmetry.[53]

In this study, novel type octa-substituted phthalocyanine derivatives [ZnPc(**3**), CuPc(**4**), and CoPc(**5**)] were prepared. The structures of synthesized phthalocyanine derivatives ZnPc(**3**), CuPc(**4**), and CoPc(**5**) were examined by taking their electronic spectra. The characteristic Q-bands of these octa-substituted phthalocyanine derivatives appeared at 674, 676, and 660 nm, respectively. As

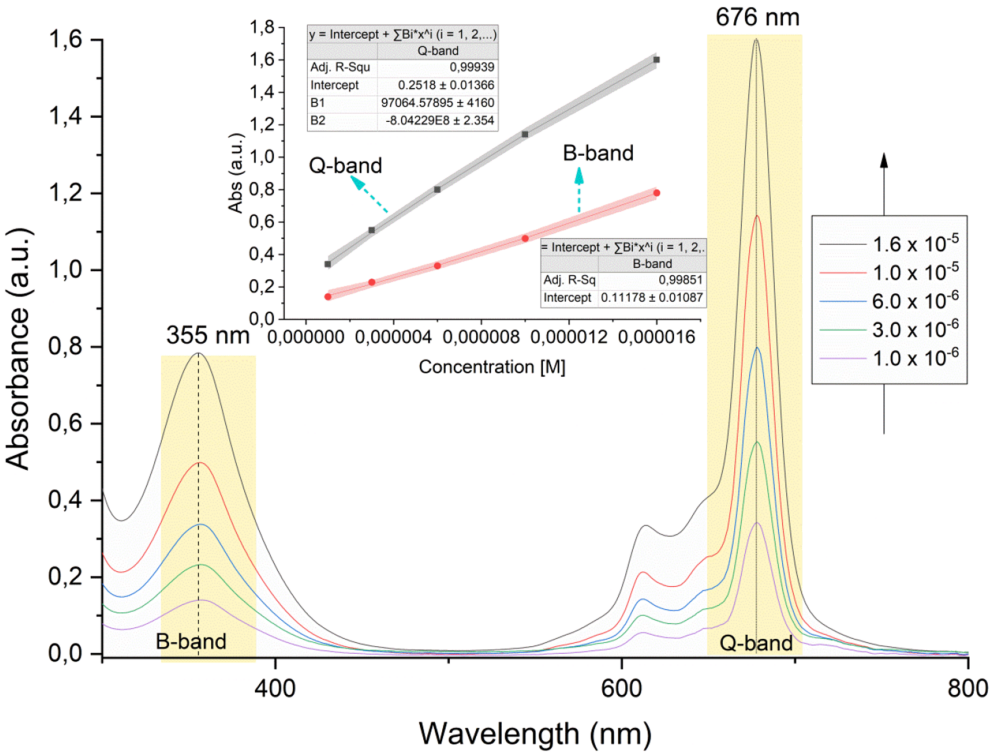

FIGURE 3 Electronic spectra of CuPc(**4**) at different concentration values (inset: the plot of Q and B-band absorbance versus concentration)

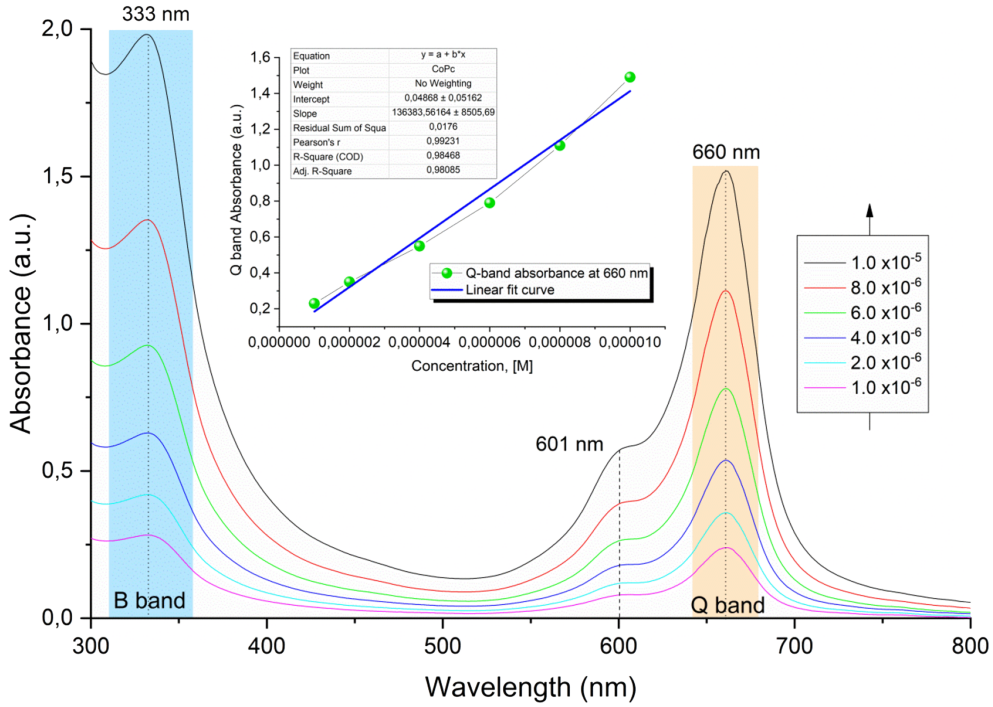

FIGURE 4 Electronic spectra of CoPc(**5**) at different concentration values (inset: the plot of Q-band absorbance versus concentration)

expected, Q-bands of phthalocyanines were obtained as a single band. The wavelength of the Q-band maxima vary depending on the metal atom at the center of the ring, and the wavelength of the max Q-band is ZnPc(**3**) > CuPc (**4**) > CoPc(**5**). The shoulder peaks of phthalocyanine compounds appeared at 613 nm for ZnPc(**3**), 615 nm for CuPc(**4**), and 601 nm for CoPc(**5**). The characteristic B-bands observed due to deeper π–π* transitions were recorded at 353, 355, and 333 nm, respectively (Figure 1).

3.3 | Aggregation properties

Phthalocyanines are known to tend to aggregate due to their conjugated 18-π electron systems. However, the

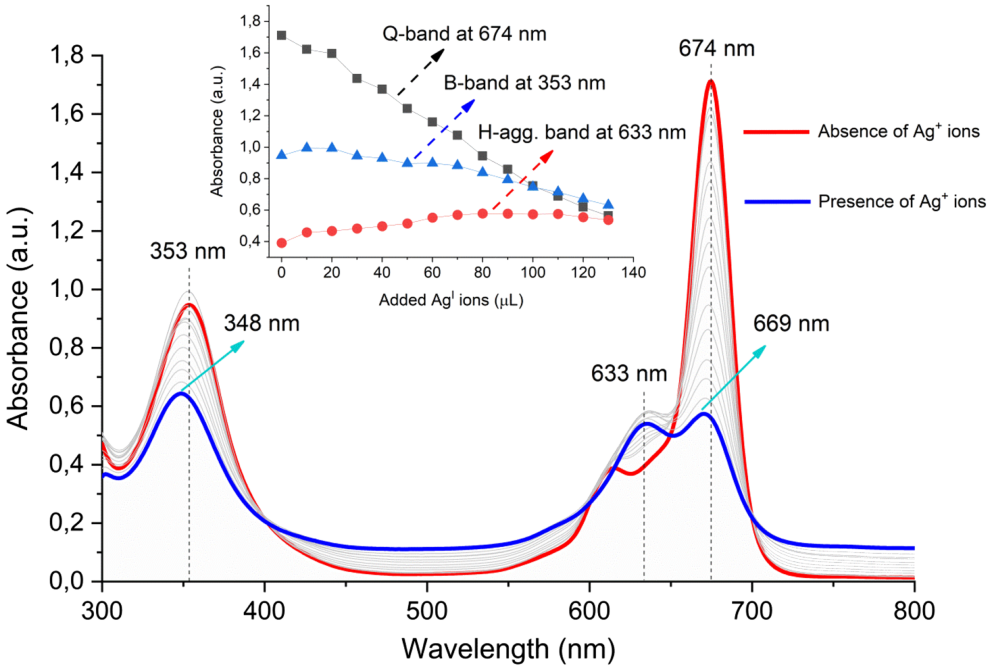

FIGURE 5 The change of ZnPc(**3**) electronic spectra during the titration with Ag^{+} ions (inset: the plot of Q-band, B-band, and H-aggregation band absorbance versus added Ag^{+} ions)

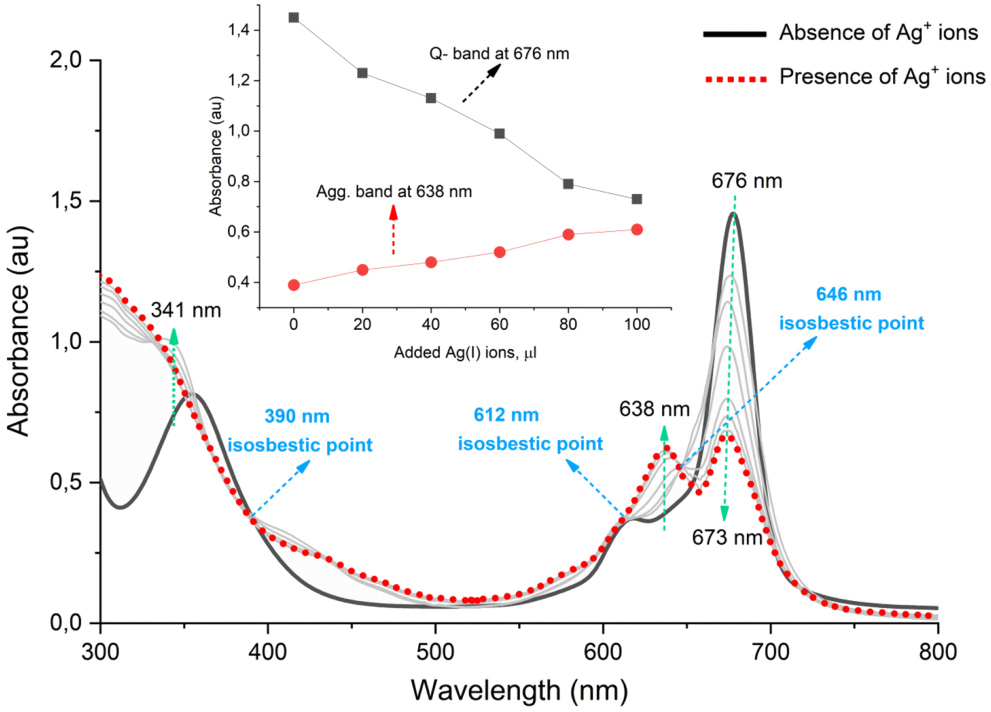

FIGURE 6 The change of CuPc(**4**) electronic spectra during the titration with Ag^{+} ions (inset: the plot of Q-band and H-aggregation absorbance versus added Ag^{+} ions)

binding of bulky groups from alpha and/or beta positions causes changes in the aggregation properties of phthalocyanines. Therefore, the aggregation behavior of newly synthesized phthalocyanines was investigated in the solution medium. The electronic spectra of the phthalocyanine solutions prepared in different concentrations were recorded. The Q- and B-bands of ZnPc(**3**), CuPc(**4**), and CoPc(**5**) increased with the increase in the concentration, and also a new absorption peak due to aggregation was not observed (Figure 2 for ZnPc(**3**), Figure 3 for CuPc(**4**), and Figure 4 for CoPc(**5**)). These results indicate that new types of octa-substituted phthalocyanines bearing 1-(4-hydroxyphenyl) propane-1-one in peripheral positions have a low tendency to aggregate at concentrations between 1 and 15 μM.

3.4 | Metal ion binding studies

Phthalocyanines can be optically sensitive to soft metal ions such as Ag(I) and Pd (II), depending on the functional group in their peripheral or nonperipheral positions. Soft metal sensitivities can be determined by UV-vis and fluorescence spectroscopy techniques. The

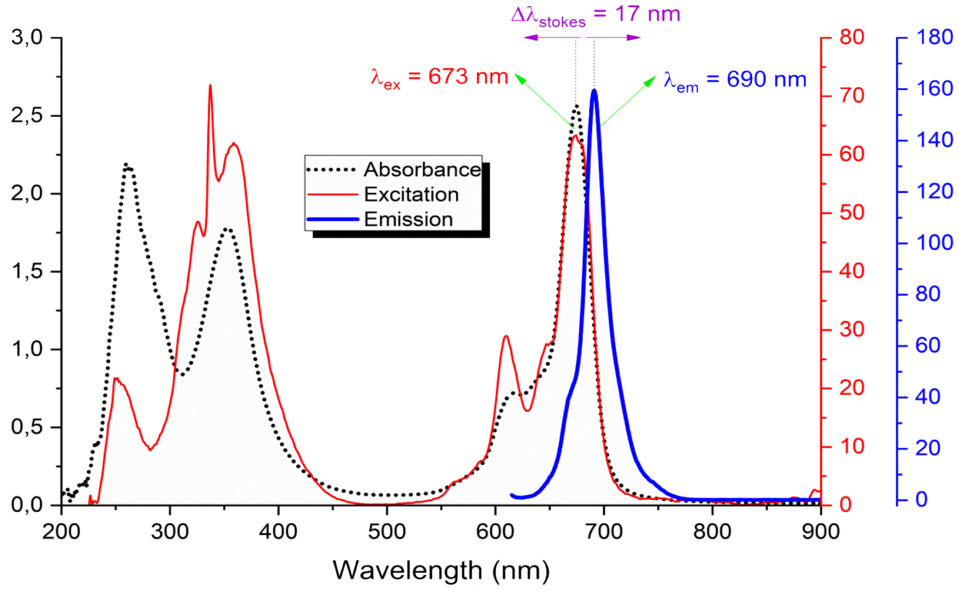

FIGURE 7 Absorbance, excitation, and emission (λ_{ex} = 600 nm) spectra of ZnPc(**3**)

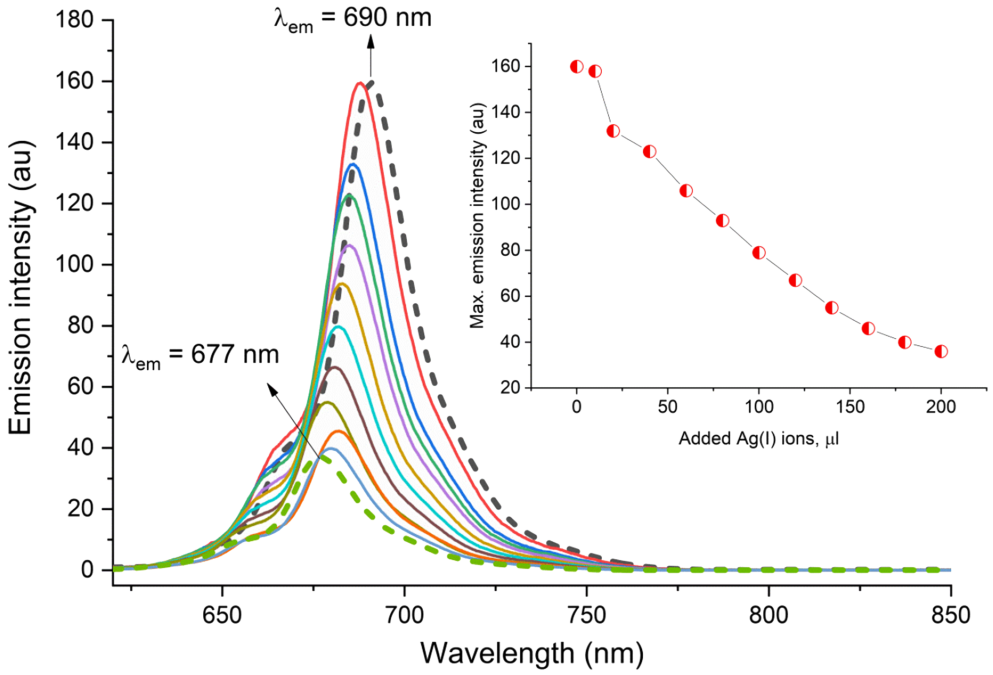

FIGURE 8 The change of fluorescence emission spectra of ZnPc(**3**) during the titration with Ag^+ ions (inset: the plot of maximum emission intensity versus added Ag^+ ions)

interaction of soft metal ions with phthalocyanines causes two types of aggregation as H-type (face to face) and J-type (edge to edge). H-type aggregation causes the Q-band to shift blue, and J-type aggregation causes it to shift to red.[54]

Optical sensitivities of newly synthesized phthalocyanine (ZnPc(**3**), CuPc(**4**), and CoPc(**5**)) toward soft metal ions were determined by recording the change of electronic spectra during the titration of about 10^{-5}-M phthalocyanine and 10^{-3}-M metal ions. The high concentration of the metal salts was chosen to eliminate the volume change. Figure 5 shows the UV-vis spectrum of ZnPc(**3**) during titration with Ag^{+} ions. The stepwise addition of Ag(I) ions caused a decrease in the Q-band at 674 nm and the B-band at 353 nm. Simultaneously, a new band was formed at 633 nm while the B-band shifted

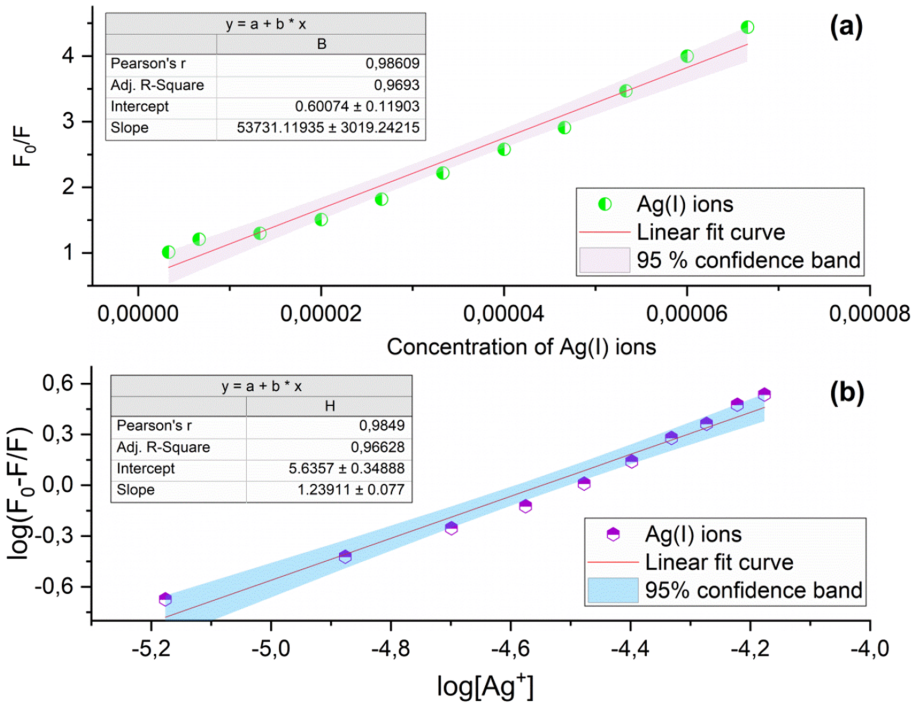

FIGURE 9 (a) Fluorescence quenching Stern–Volmer plot of ZnPc(**3**) with increasing concentration of Ag(I) ions. (b) Modified Stern–Volmer plot for Ag^{+} ions

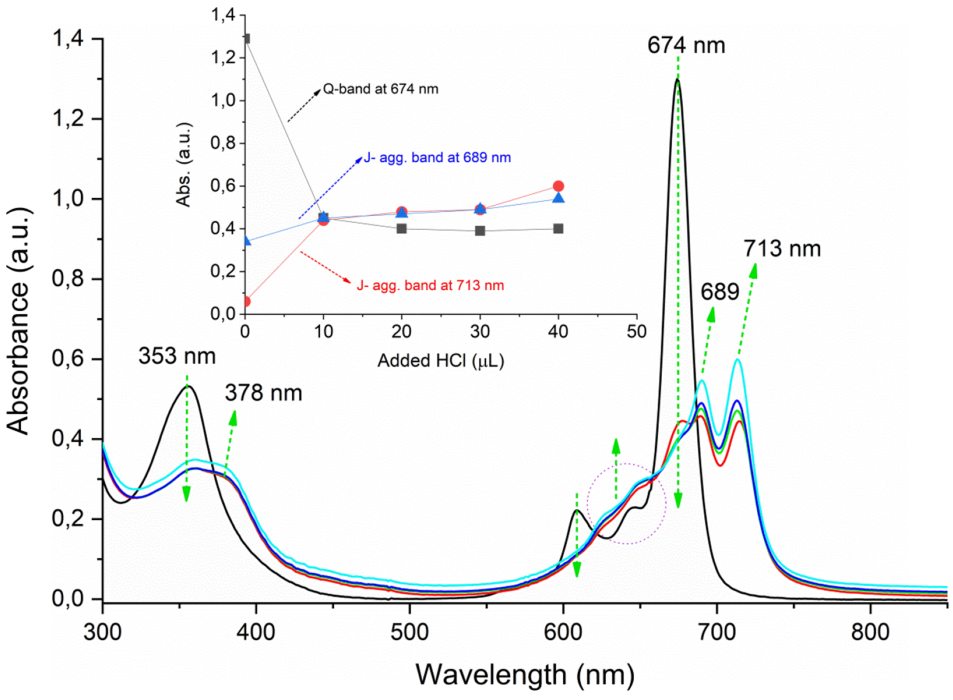

FIGURE 10 The electronic spectra of ZnPc(**3**) during the titration with HCl (Inset: The plot of Q-band and J-aggregation bands absorbance versus added HCl)

toward 348 nm due to the formation of metal-induced H-type aggregation. During titration of CuPc(**4**) with Ag^{+} ions, the Q-band intensity at 676 nm and the B-band intensity at 355 nm decreased. Simultaneously, new peaks were observed at 638 and 329 nm due to the formation of metal-induced H-type aggregation (Figure 6). The newly synthesized ZnPc(**3**) and CuPc(**4**) showed optical sensitivity to Ag(I) ions. In the titration of CoPc(**5**) with Ag^{+} ions, no significant change was observed in the electronic spectra (Figure S11).

3.5 | The results of fluorescence studies

Fluorescence properties of new type octa-substituted ZnPc(**2**) were performed in THF at room temperature. The experimental spectral parameters and photophysical results were given in Table 1. Fluorescence emission properties of CuPc(**4**) and CoPc(**5**) could not be obtained due to the paramagnetic properties. Figure 7 shows the absorption, excitation, and emission spectra of ZnPc(**3**). The fluorescence emission spectrum of ZnPc(**3**) indicates

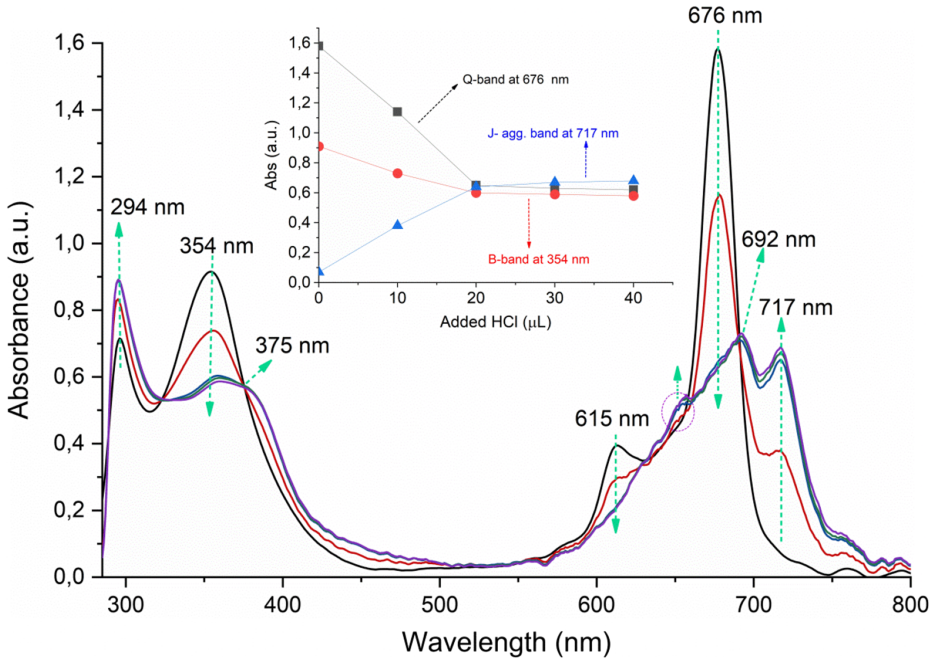

FIGURE 11 The electronic spectra of CuPc(**4**) during the titration with HCl (inset: the plot of Q-band, B-band, and J-aggregation band absorbance versus added HCl)

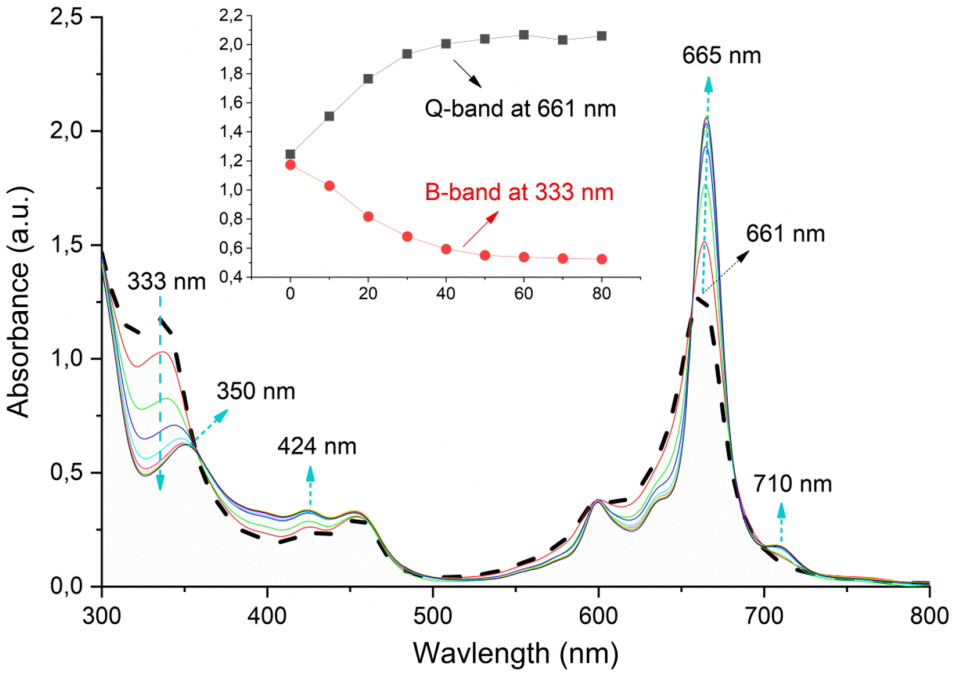

FIGURE 12 The electronic spectra of CoPc(**5**) during the titration with HCl (inset: the plot of Q-band and B-band absorbances versus added HCl)

only one emission band at 690 nm in THF ($\lambda_{ex} = 600$ nm). The absorption and excitation spectra of ZnPc(**3**) are very similar, and Q-band peaks appeared at 673 nm in both spectra. The similarity in the absorption and excitation spectrum of ZnPc(**3**) indicates that the nuclear configurations in the excited state and ground state environment are not affected by excitation in THF.[55] The fluorescence emission spectrum of ZnPc(**3**)

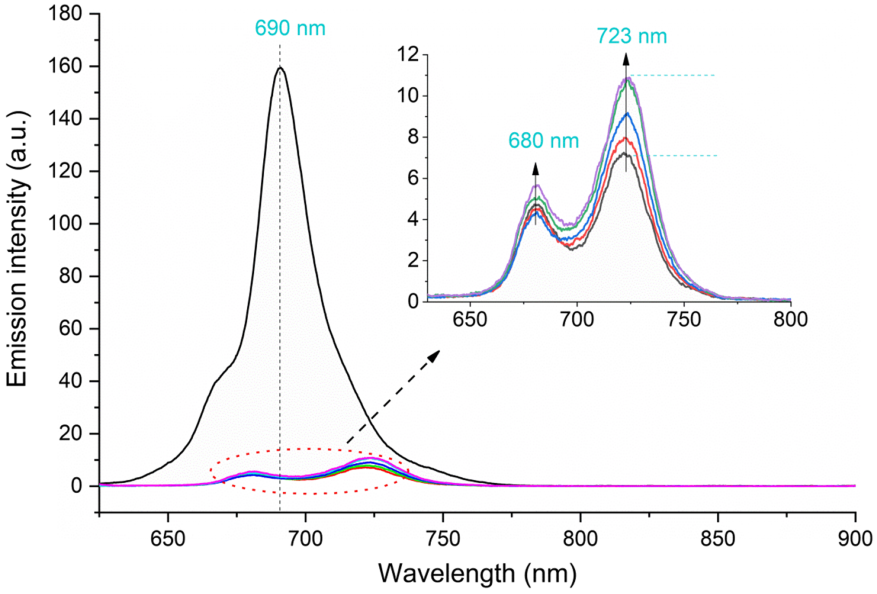

FIGURE 13 The change of emission spectrum of ZnPc(**3**) during the titration with HCl ($\lambda_{excitation} = 600$ nm) (inset: zoom emission spectra between 630 and 800 nm)

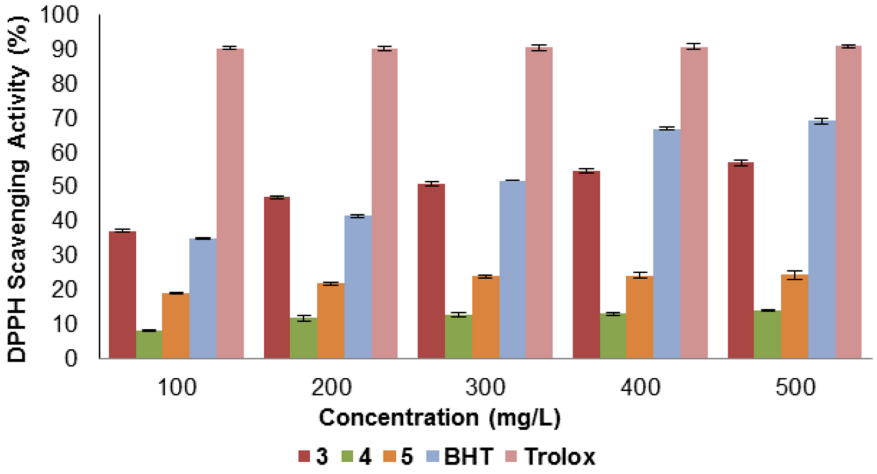

FIGURE 14 Free radical scavenging activity on DPPH radicals (%) of octa-substituted phthalocyanine derivatives ZnPc (**3**), CuPc(**4**), and CoPc(**5**), and the standards (Trolox and BHT). Vertical bars represent the SD

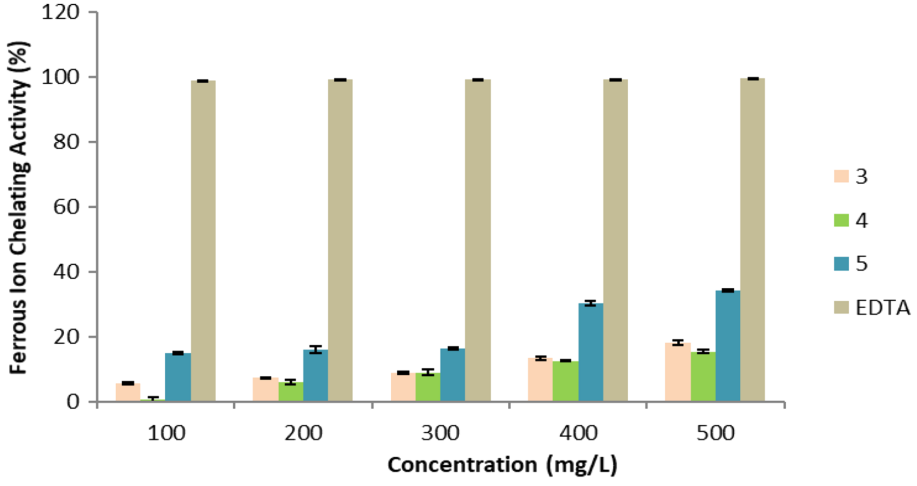

FIGURE 15 Ferrous ion chelating ability of the octa-substituted phthalocyanine derivatives ZnPc(**3**), CuPc(**4**), CoPc(**5**), and EDTA (as a standard). Vertical bars represent the SD

is the mirror image of the excitation spectrum. The obtained Stokes shift is 17 nm for ZnPc(**3**) in THF media. Fluorescence quantum yield (Φ_F) of ZnPc(**3**) was found to be 0.12 in the THF solution. Fluorescence quantum yield (Φ_F) of unsubstituted zinc phthalocyanine is 0.23 in THF. When these values are compared, octa substitution with 1-(4-hydroxyphenyl)propane-1-one groups from peripheral positions caused a decrease in fluorescence quantum yield.

The effect of Ag^+ ions on fluorescence emission spectra of novel type octa-substituted zinc phthalocyanine derivative of ZnPc(**3**) was also investigated at room temperature in THF. The changes of emission spectra during the titration with Ag^+ ions were performed. In titration experiments, the concentration of the phthalocyanine solution was used as $\approx 10^{-5}$, whereas the concentration of the solution containing Ag(I) ions was adjusted to be in the order of 10^{-3} in order to neglect the volume change. Figure 8 shows the difference in the emission spectra during the titration of octa-substituted zinc phthalocyanine with Ag^+ ions. In the absence of Ag(I) ions, the emission peak at 690 nm decreased with the incremental addition of Ag^+ ions to the medium and shifted to 677 nm with going toward blue at about 13 nm. This indicates that the HOMO-LUMO energy transition is increased due to the formation of H-type aggregation between ZnPc(**3**) and Ag(I) ions. The quenching efficiency (K_{sv}) of Ag^+ ions against octa-substituted zinc phthalocyanine was found using the Stern–Volmer equation. The binding constant (K_a) and binding stoichiometry (n) of octa-substituted zinc phthalocyanine with Ag^+ ions were calculated using the modified Benesi–Hildebrand equation. K_{sv} was found to be 5.3×10^4 mol/L. Also, K_a and n were found to be $4.32 \times 10^5\ M^{-1}$ and 1.24, respectively (Figure 9). The free energy change of octa-substituted zinc phthalocyanine in the presence of Ag^+ ions was calculated as -32.16 kJ mol^{-1}.

3.6 | The effect of protonation upon UV-vis and fluorescence spectra of phthalocyanines

The phthalocyanines that do not entirely agglomerate in a solvent environment have sharp Q-bands that are attractive for applications such as chemical sensors. Also, it is known that monoprotonated, diprotonated, and triprotonated forms of phthalocyanines cause splitting and bathochromic shifts in the Q-band due to their symmetry changes.[56] Red shifts in Q-bands give them an advantage for applications such as PDT. A study on the protonation of ZnPc with TFA and sulfuric acid obtained single and double protonated forms ($[ZnPc{\cdot}H]^+$ and $[ZnPc{\cdot}2H]^{2+}$) with TFA, whereas derivatives with concentrated sulfuric acid and triple and quaternary protons ($[ZnPc{\cdot}3H]^{3+}$ and $[ZnPc{\cdot}4H]^{4+}$) were obtained.[57]

In the light of this information, to examine proton sensor potentials, UV-vis, and fluorescence spectra of novel octa-substituted phthalocyanines (ZnPc(**3**), CuPc(**4**), and CoPc(**5**)) were measured during the titration

TABLE 2 The antibacterial activity of the novel synthesized octa-substituted phthalocyanine compounds [ZnPc(**3**), CuPc(**4**), and CoPc(**5**)] and standard antibiotic ampicillin (AMP) with inhibition diameter in millimeters

Bacteria	3	4	5	AMP
Escherichia coli (ATCC 25922)	-		8	21
Staphylococcus aureus (ATCC 25923)	13	15	13	25
Bacillus cereus (SBT8)	14	11	12	11

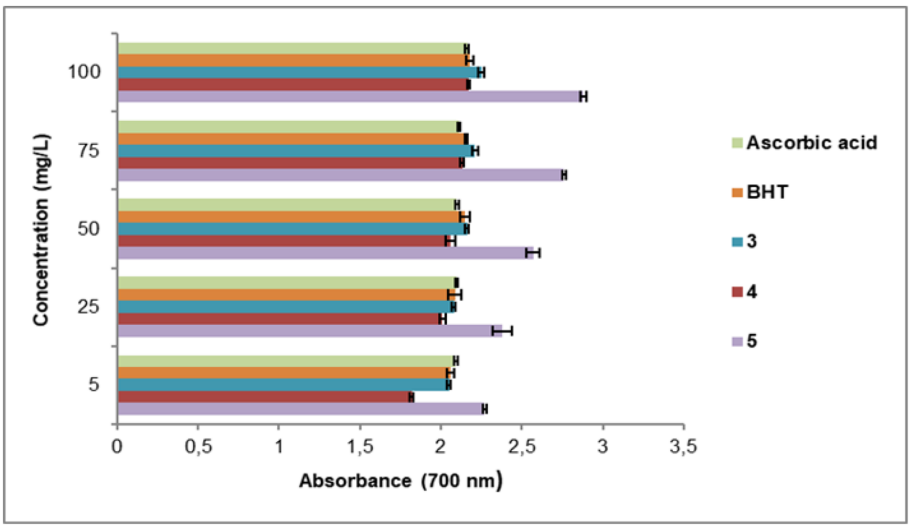

FIGURE 16 Reducing power of the octa-substituted phthalocyanine derivatives ZnPc(**3**), CuPc(**4**), CoPc(**5**), and the standards (ascorbic acid and BHT). Vertical bars represent the SD

TABLE 3 The calculated quantum chemical parameters of 4,5-bis(4-propionylphenoxy)phthalonitrile (**2**) and its octa-substituted phthalocyanine derivatives [ZnPc(**3**), CuPc(**4**), and CoPc(**5**)]

	E_{HOMO}	E_{LUMO}	I	A	ΔE	η	σ	χ	$P\dot{I}$	ω	ε	Dipole	Energy
B3LYP/6-31g level													
2	−6.8990	−2.5149	6.8990	2.5149	4.3841	2.1920	0.4562	4.7069	−4.7069	5.0536	0.1979	7.5844	−38,434.9447
3	−5.8625	−3.6455	5.8625	3.6455	2.2169	1.1085	0.9021	4.7540	−4.7540	10.1945	0.0981	2.8971	−202,158.8058
4	−5.8592	−3.6434	5.8592	3.6434	2.2158	1.1079	0.9026	4.7513	−4.7513	10.1879	0.0982	2.8709	−198,381.0188
5	−5.8619	−3.5908	5.8619	3.5908	2.2711	1.1355	0.8806	4.7264	−4.7264	9.8362	0.1017	2.8382	−191,370.2505
HF/6-31g level													
2	−8.4206	−5.1403	8.4206	5.1403	3.2804	1.6402	0.6097	6.7805	−6.7805	14.0151	0.0714	7.3267	−38,194.6242
3	−6.4560	−1.0498	6.4560	1.0498	5.4061	2.7031	0.3700	3.7529	−3.7529	2.6052	0.3838	5.7061	−201,150.5005
4	−8.0421	0.3189	8.0421	−0.3189	8.3610	4.1805	0.2392	3.8616	−3.8616	1.7835	0.5607	5.0630	−197,377.8975
5	−7.7096	0.0675	7.7096	−0.0675	7.7771	3.8885	0.2572	3.8211	−3.8211	1.8774	0.5327	4.8301	−190,369.0095
M062X/6-31g level													
2	−8.2250	−1.5630	8.2250	1.5630	6.6619	3.3310	0.3002	4.8940	−4.8940	3.5952	0.2781	7.6009	−38,419.5952
3	−6.4981	−3.0063	6.4981	3.0063	3.4918	1.7459	0.5728	4.7522	−4.7522	6.4677	0.1546	4.6580	−202,097.2948
4	−6.5033	−3.0161	6.5033	3.0161	3.4872	1.7436	0.5735	4.7597	−4.7597	6.4967	0.1539	5.2099	−198,318.7590
5	−6.5368	−2.9935	6.5368	2.9935	3.5432	1.7716	0.5645	4.7652	−4.7652	6.4085	0.1560	3.9107	−191,307.5281

with HCl. The electronic and fluorescence spectra of ZnPc(**3**), CuPc(**4**), and CoPc(**5**) were studied by a continuous variation method to examine the effects of acid addition. Figure 10 shows the spectral absorption changes observed during the protonation of ZnPc(**3**) in THF solution without HCl and the addition of HCl. With the addition of HCl, the intensity of the Q-band at 674 nm, the B-band at 353 nm, and the shoulder band at 613 nm of ZnPc(**3**) were reduced. At the same time, new peaks that shifted to red at 689 and 713 nm appeared due to the formation of J-type self-aggregation with mono protonation of ZnPc(**3**). With the addition of 40 µl of HCl, the monomers and protonated species reached equilibrium, and the addition of more acid caused little change in the spectrum. With the addition of HCl, the green color solution of ZnPc(**3**) turned pale green with detectable by the naked eye. Also, neutralization experiments were performed better to understand the effect of HCl on the electronic spectrum. A reversible electronic spectrum was obtained by titration with KOH after ZnPc (**3**) was saturated with HCl. With the addition of KOH to the mixture, the Q-band at 689 nm reappeared at the same intensity as a single band (Figure S12).

A similar titration experiment was repeated for CuPc (**4**). Figure 11 shows the changes in the electronic spectrum during titration of CuPc(**4**) with HCl. The addition of HCl upon CuPc(**4**) affected the characteristic Q- and B-bands of it. The Q-, B-, and shoulder bands of CuPc(**4**) at 676, 353, and 615 nm decreased during the addition of 40 µl of HCl. Simultaneously, the B-band at 353 nm shifted to 375 nm, and two new peaks at 692 and 717 nm appeared in the red-shifted region due to the formation of J-type self-aggregation with protonation of CuPc(**4**). Similarly, the monomers and aggregates reached equilibrium with 40 µl of HCl, and the addition of more acid caused little change in the spectrum.

In the protonation experiment of CoPc(**5**), the addition of HCl caused the Q-band to increase and shift from 661 to 665 nm, unlike the others. Although a small peak occurs around 710 nm, its intensity is lower than ZnPc(**3**) and CuPc(**4**). Also, the B-band at 333 nm shifted to 350 nm. The addition of more HCl did not cause any critical difference in the electronic spectra of CoPc(**5**) (Figure 12).

To examine the change of emission spectrum of ZnPc (**3**) with the addition of HCl, the emission spectra of

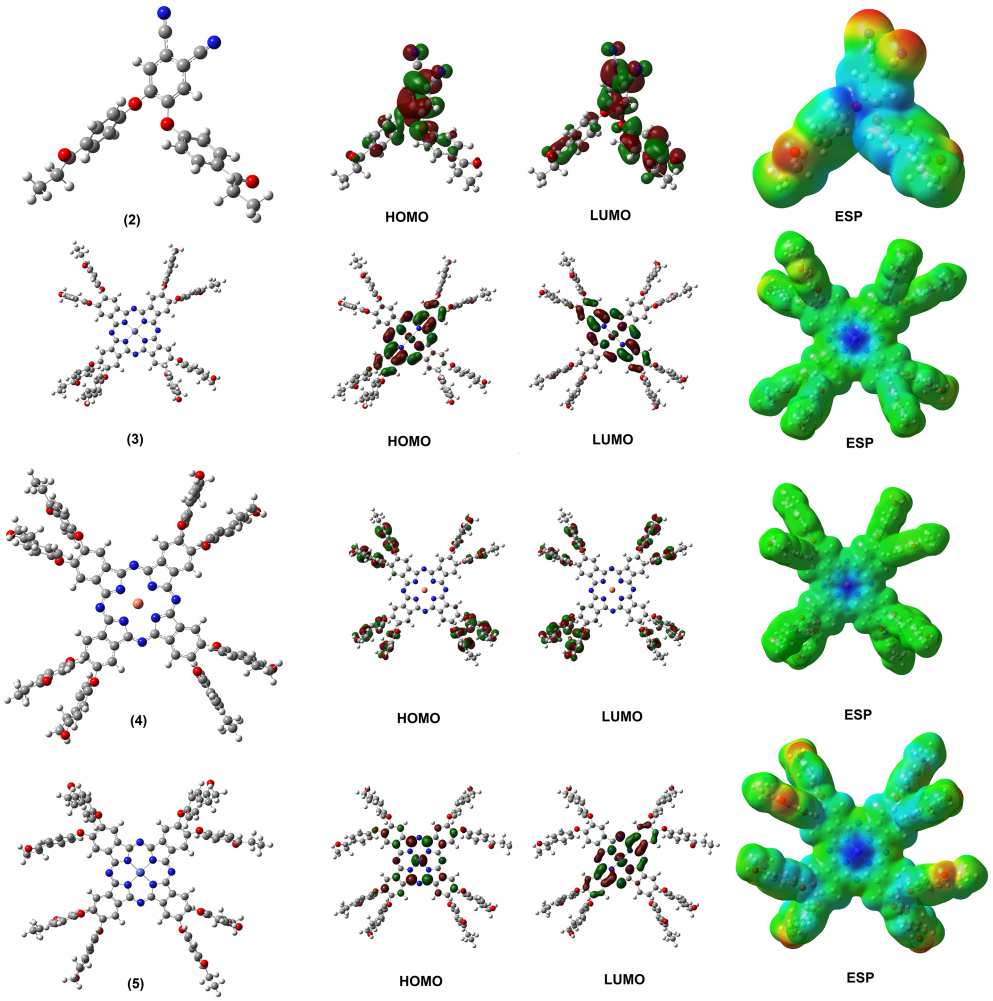

FIGURE 17
Representations of HOMO, LUMO, and ESP of 4,5-bis (4-propionylphenoxy) phthalonitrile (**2**) and its octa-substituted phthalocyanine derivatives [ZnPc(**3**), CuPc(**4**), and CoPc(**5**)]

TABLE 4 The calculated quantum chemical parameters of 4,5-bis(4-propionylphenoxy)phthalonitrile (**2**) and its octa-substituted phthalocyanine derivatives [ZnPc(**3**), CuPc(**4**), and CoPc(**5**)] in HF/6-31g level

	E_{HOMO}	E_{LUMO}	I	A	ΔE	η	σ	χ	$P\dot{I}$	ω	ε	Dipole	Energy
A protonated													
3	−9.0669	−4.1187	9.0669	4.1187	4.9482	2.4741	0.4042	6.5928	−6.5928	8.7842	0.1138	7.4612	−201,160.3282
4	−9.9015	−3.0297	9.9015	3.0297	6.8717	3.4359	0.2910	6.4656	−6.4656	6.0835	0.1644	12.2170	−197,387.2345
5	−10.6754	−2.5568	10.6754	2.5568	8.1186	4.0593	0.2463	6.6161	−6.6161	5.3917	0.1855	10.9439	−190,380.7738
Two protonated													
3	−11.5911	−7.0688	11.5911	7.0688	4.5223	2.2611	0.4423	9.3299	−9.3299	19.2484	0.0520	5.1517	−201,166.3977
4	−12.8980	−5.1166	12.8980	5.1166	7.7814	3.8907	0.2570	9.0073	−9.0073	10.4263	0.0959	3.6128	−197,395.9832
5	−12.9802	−5.1517	12.9802	5.1517	7.8285	3.9143	0.2555	9.0660	−9.0660	10.4990	0.0952	3.6895	−190,388.8497
Three protonated													
3	−13.5576	−8.9483	13.5576	8.9483	4.6094	2.3047	0.4339	11.2529	−11.2529	27.4720	0.0364	11.6538	−201,173.4360
4	−13.1862	−6.6481	13.1862	6.6481	6.5381	3.2691	0.3059	9.9171	−9.9171	15.0424	0.0665	47.5523	−197,401.0842
5	−14.2472	−8.5594	14.2472	8.5594	5.6878	2.8439	0.3516	11.4033	−11.4033	22.8622	0.0437	19.2918	−190,393.4940
Four protonated													
3	−15.0924	−11.5413	15.0924	11.5413	3.5511	1.7756	0.5632	13.3168	−13.3168	49.9386	0.0200	5.4086	−201,176.5940
4	−15.0807	−9.6394	15.0807	9.6394	5.4412	2.7206	0.3676	12.3601	−12.3601	28.0765	0.0356	39.5092	−197,404.1271
5	−15.1517	−11.0316	15.1517	11.0316	4.1201	2.0601	0.4854	13.0916	−13.0916	41.5987	0.0240	8.0789	−190,391.6976

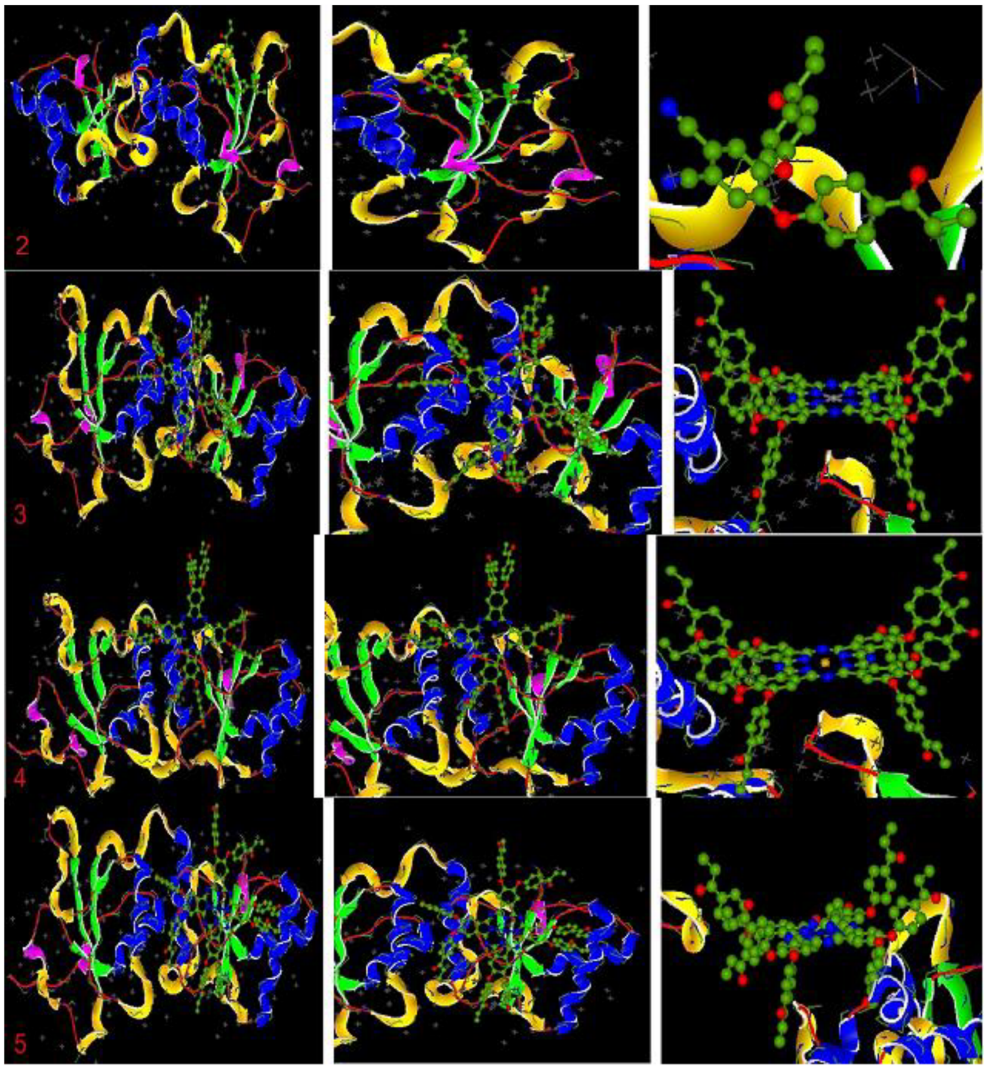

FIGURE 18 Representation of 4,5-bis(4-propionylphenoxy) phthalonitrile (**2**) and its octa-substituted phthalocyanine derivatives [ZnPc(**3**), CuPc(**4**), and CoPc(**5**)] with breast cancer

ZnPc(**3**) were recorded by the stepwise addition of HCl. Figure 13 shows the change in emission spectra during the titration of ZnPc(**3**) with HCl. The addition of 10 µl of HCl upon ZnPc(**3**) resulted in quenching the emission peak at 690 nm. At the same time, new shoulder-shaped peaks at 680 and 723 nm occurred. The addition of up to 50 µl of acid caused to rise slightly of these peaks. But adding more acid did not change significantly in the emission spectrum.

3.7 | Antioxidant and antibacterial properties

3.7.1 | DPPH radical scavenging activity

The DPPH radical scavenging activity method is a widely used method that provides results to achieve the antioxidant properties of natural and synthetic antioxidant compounds in a relatively short time. In the present study, DPPH radical scavenging activities of the synthesized octa-substituted phthalocyanine derivatives ZnPc(**3**), CuPc(**4**), and CoPc(**5**), and the standards (Trolox and BHT) were determined and presented in Figure 14). The DPPH radical scavenging activity tests were applied to the Pc compounds in DMSO. The results are shown as a percentage of the absorbance decrease of the DPPH radical at different concentrations of the phthalocyanine compounds tested. The order of radical scavenging effects of the Pc compounds were **3** > **5** > **4** at the same concentrations. However, all tested metallophthalocyanine compounds showed lower DPPH activity than the BHT and Trolox standards except compound **3** (Figure 12). Among the compounds, maximum radical scavenging activity was 37.30% for Pc compound **3** at 100 mg/ml. It had almost similar activity to the BHT standard at any concentration tested but lower than the Trolox standard at the concentrations evaluated. The results of DPPH scavenging activities of the tested phthalocyanine compounds were also exposed to good agreement with literature and prior reports.[58]

3.7.2 | Ferrous ion chelating activity

Ferrous ion (Fe^{2+}) is a transition metal ion among many transition metals that cause the formation of harmful reactive oxygen species (ROS) and free radicals, which are dangerous for living organisms. ROS are powerful oxidizing molecules and can cause permanent cell damage, organ failure, diseases such as cancer, and even death in cells and living organisms. To prevent the formation of these harmful compounds, antioxidant substances and especially the compounds that chelate metal ions are used.[59] In the present work, ferrous ion chelating activities of the synthesized metallophthalocyanine compounds, and EDTA, which is an excellent chelating compound as a standard, were examined. The results were indicated in Figure 15. The chelating activities were $30.21 \pm 0.22\%$, $34.08 \pm 0.41\%$ and $41.34 \pm 0.63\%$ for **4**, **3**, and **5**, respectively, at 500 μg ml^{-1} concentration. When the chelating activities of the compounds were evaluated with each other and EDTA, compound **5** had slightly higher activity than other synthesized metallophthalocyanine derivatives. However, all synthesized octa-substituted metallophthalocyanine derivatives had lower chelating activity than EDTA as a standard at all concentrations. The results in this work are in parallel with similar studies in the literature.[60]

3.7.3 | Reducing power activity

One of the most widely used antioxidant methods to evaluate the antioxidant properties of natural and synthetic compounds is the reducing power method. The method is based on the principle that compounds having reducing potential can react with potassium ferricyanide ($K_3Fe^{3+}(CN)_6$) to give potassium ferrocyanide ($K_4Fe^{2+}(CN)_6$). Then, it can react with demir(III)chloride ($FeCl_3$) to give a ferric–ferrous complex. This reaction can be observed by the color change from green to blue depending on the reduction power capacity of the antioxidant compound at 700 nm.[61]

In this study, the newly synthesized phthalocyanine compounds in DMSO were analyzed for their reducing power ability. BHT and ascorbic acid were preferably used as positive standards. All results were illustrated in Figure 16. According to the results, all tested Pc

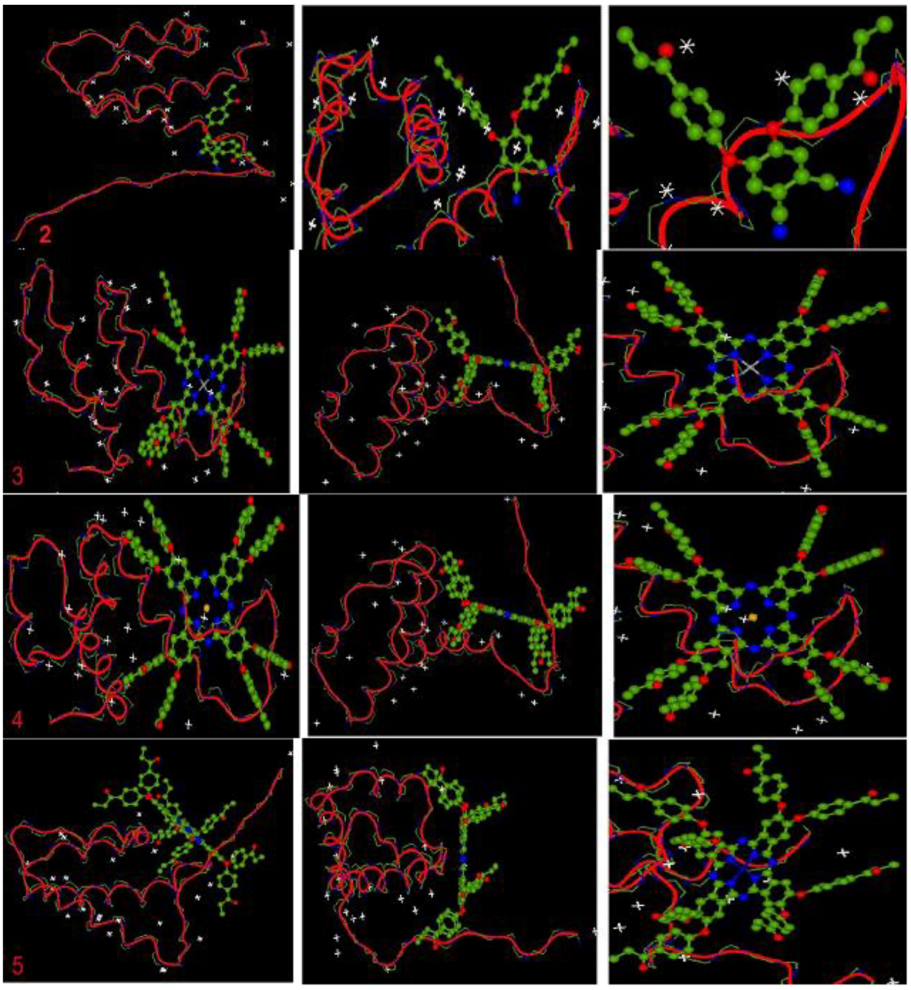

FIGURE 19 Representation of 4,5-bis(4-propionylphenoxy) phthalonitrile (**2**) and its octa-substituted phthalocyanine derivatives [ZnPc(**3**), CuPc(**4**) and CoPc(**5**)] with liver cancer

compounds showed very good reducing power activity, in the order compound: **5** (2.88 ± 0.01) > **3** (2.25 ± 0.01) > **4** (2.17 ± 0.02) ≈ BHT (2.18 ± 0.01) > ascorbic acid (2.16 ± 0.008). However, all Pc compounds synthesized except **4**, which had similar reducing power activity with the standards, showed much higher reducing power than both standard compounds (BHT and ascorbic acid) at any concentrations. Additionally, compound **5**, in particular, showed an excellent result in reducing power activity among other Pc compounds. The observed results are similar to those in the previous works.[62,63]

3.7.4 | Antibacterial properties

The antibacterial properties of the synthesized Pc compounds were analyzed by using agar well diffusion method. For this experiment, three different bacterial species were used. They were gram-negative (*E. coli*) and gram-positive (*S. aureus* and *B. cereus*) bacteria. The antibacterial activity results were illustrated in Table 2. According to the results, the newly synthesized metallophthalocyanine compounds showed antibacterial activity against all bacteria tested with 8- to 15-mm inhibition zones (Figures S13–S15). Furthermore, DMSO as a controlled solvent had no inhibitory effect on the bacteria tested. All synthesized compounds showed a good inhibitor effect against gram-positive bacteria *S. aureus* and *B. cereus* (SBT8) with inhibition diameters of 11–15 mm.

TABLE 5 E total energy values of 4,5-bis(4-propionylphenoxy) phthalonitrile (**2**) and its octa-substituted phthalocyanine derivatives [ZnPc(**3**), CuPc(**4**), and CoPc(**5**)]

	Breast cancer	Liver cancer	Lung cancer
2	−304.14	−351.82	−305.30
3	−501.48	−609.72	−526.75
4	−504.26	−590.48	−484.18
5	−560.21	−607.04	−513.63

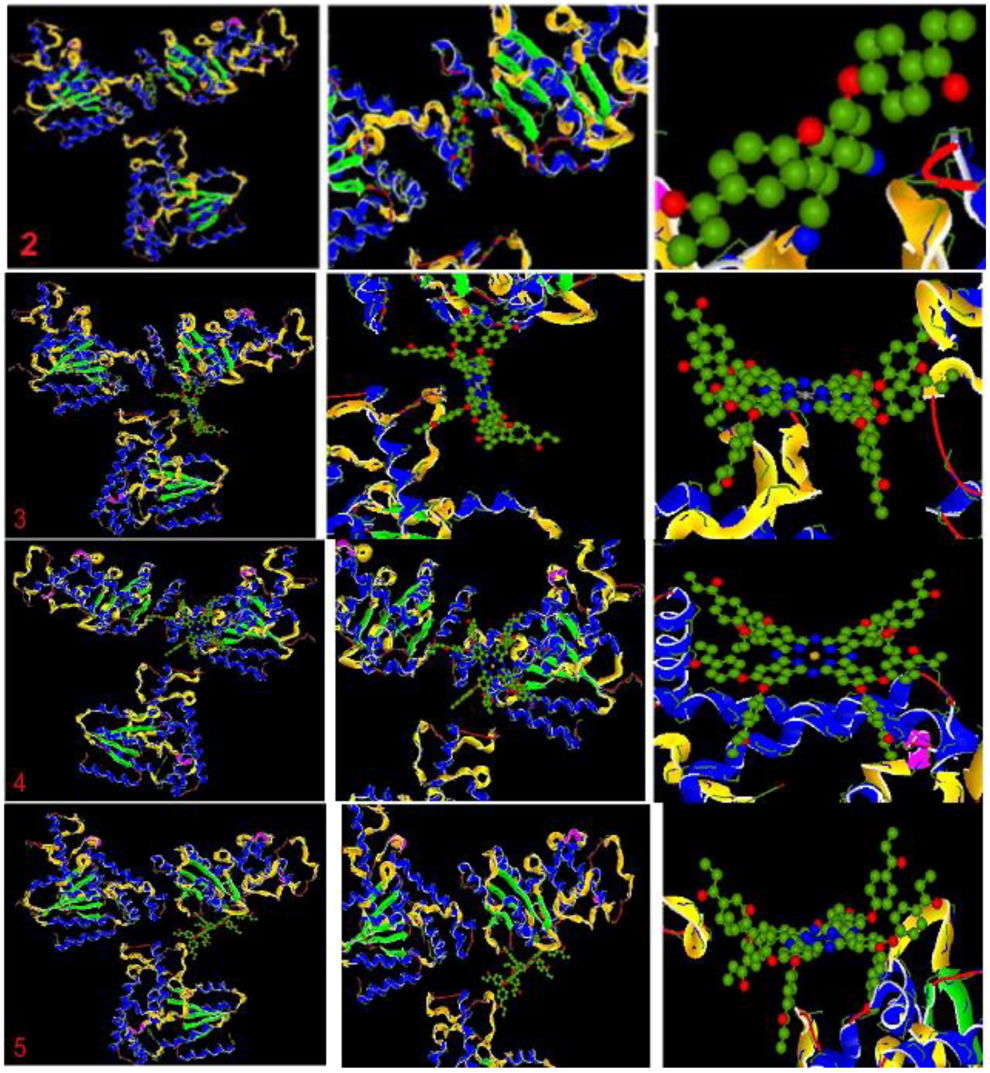

FIGURE 20 Representation of 4,5-bis (4-propionylphenoxy) phthalonitrile (**2**) and its octa-substituted phthalocyanine derivatives [ZnPc(**3**), CuPc(**4**), and CoPc(**5**)] with lung cancer

However, compound **3** did not show any inhibitory effect against *E. coli*, but compounds **4** and **5** had an inhibitory effect against gram-negative bacteria *E. coli* with an inhibition zone of 9 and 8 mm. Overall, the synthesized octa-substituted phthalocyanine compounds in DMSO had good antibacterial effects against all tested bacteria. Our results were similar to several studies about the antibacterial activities of the phthalocyanine compounds.[64–67]

3.8 | Theoretical results

Nowadays, theoretical calculations are becoming very common and developing day by day. Theoretical calculations give the chemical activities of molecules in a short time and provide significant savings.[68] Also, the active regions of the molecules can be easily determined by theoretical calculations. In this way, it is possible to design more active and more effective molecules. Recent studies have shown that it has become complicated to develop more active and effective molecules. Experimental studies reveal that metal complexes were more practical and functional than ligand molecules. Therefore, it is crucial that investigate metal complexes with theoretical calculations.[46]

As a result of the calculations made with the Gaussian software program, many quantum chemical parameters have been found. All parameters found are given in Table 3. Among these parameters, the two most important and most obvious of the molecules are HOMO that is the highest occupied molecular orbital, and LUMO that is the lowest unoccupied molecular orbital. The HOMO parameter is used to explain the chemical activities of the molecules. The molecule with the most positive numerical value of this parameter has the highest chemical activity.[68] On the other hand, the chemical activity of the molecule with the lowest

TABLE 6 Hydrophobic Interactions of protein with octa-substituted zinc and cobalt phthalocyanines [ZnPc(**3**) and CoPc(**4**)]

Index	Residue	AA	Distance	Ligand atom	Protein atom
Breast cancer—CoPc					
1	6A	HIS	3.28	1354	92
2	7A	HIS	3.18	1311	109
3	11A	LEU	3.59	1353	158
4	17A	GLN	3.82	1369	247
5	18A	GLU	3.11	1287	263
6	18A	GLU	3.68	1301	264
7	20A	GLU	3.26	1487	297
8	21A	ALA	2.73	1364	312
9	22A	LYS	3.27	1289	323
Liver cancer—ZnPc					
1	1649X	ARG	3.37	2027	5
2	1649X	ARG	3.48	2151	5
3	1669X	ALA	2.36	2168	190
4	1670X	ARG	3.61	2168	196
5	1676X	LEU	3.92	2045	250
6	1678X	ASN	3.25	1998	268
7	1679X	LEU	2.89	2071	282
8	1679X	LEU	2.26	2001	281
9	1679X	LEU	3.07	2000	280
10	1681X	THR	2.01	1989	299
11	1683X	GLU	2.51	1976	317
12	1776X	PRO	3.71	2140	1155
Lung cancer proteins—ZnPc					
1	504B	VAL	3.92	7316	2101

Abbreviations: ALA, alanine; ARG, arginine; ASN, asparagine; GLN, glutamine; GLU, glutamic acid; HIS, histidine; LEU, leucine; LYS, lysine; PRO, proline; THR, threonine; VAL, valine.

numerical value of the LUMO parameter of the molecules is also high.[42] These parameters are important parameters used to explain intermolecular electron transfer. In the calculations made, the numerical value of the HOMO parameter of ZnPc(**3**) is generally more positive than the others. Therefore, the chemical activity of ZnPc (**3**) is higher than the others. On the other hand, the numerical value of the LUMO parameter of ZnPc(**3**) is generally more negative than the others. As a result, the chemical activity of ZnPc(**3**) is higher than the others. Apart from these two parameters, many parameters are calculated, such as I, A, ΔE, η, σ, χ, $P\dot{I}$, ω, ε, dipole, and energy. All of these parameters are calculated from the HOMO and LUMO parameters of the molecule. Figure 17 shows the visual representation of HOMO, LUMO, and ESP (electrostatic potential) for 4,5-bis (4-propionylphenoxy)phthalonitrile (**2**) and its octa-substituted phthalocyanine derivatives [ZnPc(**3**), CuPc (**4**), and CoPc(**5**)].

It has been seen in the literature review that it is seen that phthalocyanine protonated by a strong acid from the nitrogen atom in meso positions. Again in this study, it was observed that the stability of metal phthalocyanines against acids increased in the following order: ZnPc < CuPc < CoPc.[22,56] In the theoretical studies, HOMO and LUMO energy values are used to evaluate the stability of the molecule. To perform stability of novel synthesized octa-substituted metallophthalocyanines [ZnPc(**3**), CuPc(**4**), and CoPc(**5**)] in acidic media, they were protonated four times, respectively. HOMO and LUMO energy values of the octa-substituted metallophthalocyanines progressed to more negative values in each protonation ((Figure S16 for ZnPc(**3**), Figure S17 for CuPc(**4**), and Figure S18 for CoPc(**5**). The obtained all chemical parameters for protonated phthalocyanines derivatives were summarized in Table 4.

It is well known that theoretical methods are used to compare the chemical and biological activities of novel drug compounds recently. Therefore, the biological activities of 4,5-bis(4-propionylphenoxy)phthalonitrile (**2**) and its octa-substituted phthalocyanine derivatives [ZnPc(**3**), CuPc(**4**), and CoPc(**5**)] against cancer proteins were compared with molecular docking studies. As a result of the calculations, the most critical parameter is the E total parameter. The molecule with the most negative numerical value of this parameter has the highest biological activity. Figures 18–20 show that the interactions of 4,5-bis(4-propionylphenoxy)phthalonitrile (**2**) and its octa-substituted phthalocyanine derivatives [ZnPc(**3**), CuPc(**4**), and CoPc(**5**)] with some cancer proteins (Figure 18 for lung cancer, Figure 19 for liver cancer, and Figure 20 for breast cancer proteins).

The main factor determining the numerical value of the E total parameter is the interactions between molecules and proteins. There are many interactions such as hydrogen bonds, polar and hydrophobic interactions, π–π, and halogen, between molecules and proteins.[69,70] An increase of interaction between molecules and

TABLE 7 Hydrogen bonds of protein with octa-substituted zinc and cobalt phthalocyanines [ZnPc(**3**) and CoPc(**4**)]

Index	Residue	AA	Distance H-A	Distance D-A	Donor angel
Breast cancer—CoPc					
1	8A	SER	1.72	2.58	140.36
2	17A	GLN	3.42	4.02	119.40
3	22A	LYS	2.93	3.90	159.18
4	38A	GLN	1.72	2.57	138.25
Liver cancer—ZnPc					
1	1650X	MET	2.68	3.44	132.66
2	1677X	THR	2.99	3.75	138.65
3	1678X	ASN	1.51	2.40	144.70
4	1678X	ASN	2.93	3.91	167.76
5	1681X	THR	2.43	3.25	144.71
6	1683X	GLU	2.74	3.58	148.93
Lung cancer proteins—ZnPc					
1	480B	LYS	3.44	3.79	102.79
2	481B	GLU	2.51	2.96	106.99
3	513B	HIS	3.40	3.74	101.98

Abbreviations: ASN, asparagine; GLN, glutamine; GLU, glutamic acid; HIS, histidine; LYS, lysine; MET, methionine; PRO, proline; SER, serine; THR, threonine.

proteins significantly changes the value of the E total parameter; as a result of this, the biological activities of the molecules also increase. The E total parameter of compound (**2**) and its octa-substituted phthalocyanine derivatives [ZnPc(**3**), CuPc(**4**), and CoPc(**5**)] for breast cancer, liver cancer, and lung cancer proteins are summarized in Table 5. The values of the E total parameter of ZnPc(**3**), CuPc(**4**), and CoPc(**5**) are about two times higher compared with the 4,5-bis(4-propionylphenoxy) phthalonitrile (**2**).

Figures S19–S21 show that schematic illustrations of the interactions between protein and octa-substituted phthalocyanine derivatives [ZnPc(**3**), CuPc(**4**), and CoPc (**5**)]. There are many interactions, such as hydrophobic interactions and hydrogen bonds in protein–phthalocyanine. Some properties such as distances and angles were examined, and obtained dates were given in Tables 6 and 7.

4 | CONCLUSION

Within the scope of this study, we have prepared 4,5-bis (4-propionylphenoxy)phthalonitrile (**2**) and its octa-substituted phthalocyanine derivatives [ZnPc(**3**), CuPc (**4**), and CoPc(**5**)]. The newly synthesized phthalocyanines showed nonaggregation behaviors in THF media. The ZnPc(**3**) and CuPc(**4**) showed H-type aggregation toward Ag^+ ions. The compound CoPc(**5**) did not show interesting optically sensitivity toward Ag^+ ions in electronic spectra. Besides them, target octa-substituted phthalocyanines showed interesting behavior during the titration with acid. Significantly, Q-bands of ZnPc(**3**) and CuPc(**4**) shifted to the red about 40 nm during the addition of acid due to protonation. The titration of CoPc(**5**) with HCl was caused to the enhancement of Q-band intensity. Besides, synthesized octa-substituted metallophthalocyanine compounds have good antioxidant and antibacterial properties. According to the radical scavenging activity on the DPPH radical, the highest activity was achieved with ZnPc(**3**); even at the same concentrations, it had similar activity to the BHT standard. CoPc(**5**) compound had better iron ion chelating activity than others. All synthesized novel octa-substituted metallophthalocyanines showed extreme reducing power activities. Even among others, CoPc(**5**) had much better-reducing power activity than both standards (BHT and ascorbic acid). Moreover, the new Pc compounds showed better antibacterial activity against *S. aureus*, *B. cereus* than *E. coli* bacteria. The comparison of chemical and biological activities of 4,5-bis(4-propionylphenoxy) phthalonitrile (**2**) and its octa-substituted phthalocyanine derivatives [ZnPc(**3**), CuPc(**4**), and CoPc(**5**)] were made by theoretical calculations. As a result of both Gaussian software calculations and molecular docking calculations, it has been found that the ZnPc(**3**) is generally more active and effective than the others.

ACKNOWLEDGMENT

This work was supported by the Scientific and Technological Research Council of Turkey (TUBITAK), Grant/Award Number: 116Z052.

AUTHOR CONTRIBUTIONS

Ahmet T. Bilgiçli: Conceptualization; data curation; formal analysis; investigation; methodology; supervision; visualization. **Tugberk Kandemir:** Data curation; formal analysis; investigation; resources. **Burak Tüzün:** Investigation; methodology; software; visualization. **Rana Arıduru:** Data curation; formal analysis; investigation. **Armağan Günsel:** Data curation; formal analysis; investigation; methodology. **Çağla Abak:** Data curation; formal analysis; investigation; methodology. **M. Nilüfer Yarasir:** Conceptualization; data curation; investigation; methodology; resources. **Gulnur Arabaci:** Conceptualization; data curation; investigation; methodology; visualization.

DATA AVAILABILITY STATEMENT

The data that support the findings of this study are available from the corresponding author upon reasonable request.

ORCID

Tugberk Kandemir https://orcid.org/0000-0003-2084-3577
Burak Tüzün https://orcid.org/0000-0002-0420-2043
Rana Arıduru https://orcid.org/0000-0001-6852-4474
Armağan Günsel https://orcid.org/0000-0003-1965-1017
Çağla Abak https://orcid.org/0000-0002-8596-7039
M. Nilüfer Yarasir https://orcid.org/0000-0002-7327-7137
Gulnur Arabaci https://orcid.org/0000-0002-1190-5695

REFERENCES

[1] K. Gold, B. Slay, M. Knackstedt, A. K. Gaharwar, *Advanced Therapeutics* **2018**, *1*(3), 1700033.
[2] F. C. Tenover, *Am J Infect Control* **2006**, *34*, 1.
[3] J. Lemire, J. J. Harrison, R. J. Turner, *Nat Rev Microbiol* **2013**, *11*, 371.
[4] A. T. Bilgicli, H. Genç Bilgicli, A. Günsel, H. Pişkin, B. Tüzün, M. N. Yarasir, M. Zengin, *J. Photochem. Photobiol., A* **2020**, *389*, 112287.
[5] M. Sönmez, İ. Berber, E. Akbaş, *Eur. J. Med. Chem.* **2006**, *41*, 101.
[6] A. Frei, *Antibiotics (Basel)* **2020**, *9*(2), 90.

[7] R. J. Turner, *Microb. Biotechnol.* **2017**, *10*(5), 1062.
[8] N. Saki, M. Akin, A. Atsay, H. R. Pekbelgin Karaoglu, M. Burkut Kocak, *Inorg. Chem. Commun.* **2018**, *95*, 122.
[9] M. S. Ağırtaş, D. G. Solgun, S. Özdemir, M. S. İzgi, *ChemistrySelect* **2018**, *3*, 3523.
[10] M. Aydın, E. H. Alıcı, A. T. Bilgiçli, M. N. Yarasir, G. Arabaci, *Inorg. Chim. Acta* **2017**, *464*, 1.
[11] M. Á. Revuelta-Maza, P. González-Jiménez, C. Hally, M. Agut, S. Nonell, G. de la Torrea, T. Torres, *Eur. J. Med. Chem.* **2020**, *187*, 111957.
[12] C. I. Abuajah, A. C. Ogbonna, C. M. Osuji, *J. Food Sci. Technol.* **2015**, *52*, 2522.
[13] D. A. Vaibhav, W. Arunkumar, M. P. Abhijit, S. Arvind, *Int J. Curr. Pharm. Res.* **2011**, *1*, 8.
[14] X. Li, B.-D. Zheng, X.-H. Peng, S.-Z. Li, J.-W. Ying, Y. Zhao, J.-D. Huang, J. Yoon, *Coord. Chem. Rev.* **2019**, *379*, 147.
[15] G. de la Torre, P. Vázquez, F. Agulló-López, T. Torres, *Chem. Rev.* **2004**, *104*(9), 3723.
[16] E. H. Alici, A. T. Bilgiçli, A. Günsel, G. Arabaci, M. N. Yarasir, *Dalton Trans.* **2021**, *50*, 3224.
[17] M. Urbani, M. E. Ragoussi, M. K. Nazeeruddin, T. Torres, *Coord. Chem. Rev.* **2019**, *381*, 1.
[18] J. J. Cid, M. García-Iglesias, J. H. Yum, A. Forneli, J. Albero, E. Martínez-Ferrero, P. Vazquez, M. Gratzel, M. K. Nazeeruddin, E. Palomares, T. Torres, *Chem. – Eur. J.* **2009**, *15*(20), 5130.
[19] A. T. Bilgiçli, A. Günsel, M. Kandaz, A. R. Özkaya, *Dalton Trans.* **2012**, *41*, 7047.
[20] Y. C. Yang, J. R. Ward, R. P. Seiders, *Inorg. Chem.* **1985**, *24*, 1765.
[21] E. J. Osburn, L. K. Chau, S. Y. Chen, N. Collins, D. F. O'Brien, *Langmuir* **1996**, *12*(20), 4784.
[22] F. Bächle, C. Maichle-Mössmer, T. Ziegler, *ChemPlusChem* **2019**, *84*, 1081.
[23] A. Günsel, E. Güzel, A. T. Bilgiçli, G. Yaşa Atmaca, A. Erdoğmuş, M. N. Yarasir, *J. Lumin.* **2017**, *192*, 888.
[24] C. Hepokur, A. Günsel, M. N. Yarasir, A. T. Bilgiçli, B. Tüzün, G. Tüzün, İ. Yaylim, *RSC Adv.* **2017**, *7*, 56296.
[25] M. Erdoğan, P. Taslimi, B. Tuzun, *Arch. Pharm.* **2021**, *354*, e2000409.
[26] E. Önem, B. Tüzün, S. Akkoç, *J. Biomol. Struct. Dyn.* **2021**, 1.
[27] R. S. Williams, R. Green, J. M. Glover, *Nat. Struct. Biol.* **2001**, *8*(10), 838.
[28] J. Anantharajan, H. Zhou, L. Zhang, T. Hotz, M. Y. Vincent, M. A. Blevins, C. Kang, *Mol. Cancer Ther.* **2019**, *18*(9), 1484.
[29] H. Li, K. L. Fung, D. Y. Jin, S. S. Chung, Y. P. Ching, I. O. L. Ng, H. Sun, *Proteins: Struct., Funct., Bioinf.* **2007**, *67*(4), 1154.
[30] S. Frey-Forgues, D. Lavabre, *J. Chem. Educ.* **1999**, *76*, 1260.
[31] A. Günsel, E. Kirbaç, B. Tüzün, A. Erdoğmuş, A. T. Bilgiçli, M. N. Yarasir, *J. Mol. Struct.* **2019**, *1180*, 127.
[32] E. T. Saka, M. Durmuş, H. Kantekin, *J. Organomet. Chem.* **2011**, *696*, 913.
[33] T. Arslan, M. Umutlu, O. Güney, *Journal of Fluorescence* **2020**, *30*, 365.
[34] M. S. Blois, *Nature* **1958**, *181*, 1199.
[35] T. C. P. Dinis, V. M. C. Madeira, L. M. Almeida, *Arch. Biochem. Biophys.* **1994**, *315*, 161.
[36] M. Oyaizu, *Jpn. J. Nutr.* **1986**, *44*, 307.
[37] C. Valgas, S. M. De Souza, E. F. A. Smânia, *Braz. J. Microbiol.* **2007**, *38*, 369.
[38] R. Dennington, T. Keith, J. Millam, *GaussView, Version 6*, Semichem Inc. **2016**.
[39] Chemissan Version 4.43 package (**2016**)
[40] M. J. Frisch, G. W. Trucks, H. B. Schlegel, G. E. Scuseria, M. A. Robb, J. R. Cheeseman, G. Scalmani, V. Barone, B. Mennucci, G. A. Petersson, H. Nakatsuji, M. Caricato, X. Li, H. P. Hratchian, A. F. Izmaylov, J. Bloino, G. Zheng, J. L. Sonnenberg, M. Hada, M. Ehara, K. Toyota, R. Fukuda, J. Hasegawa, M. Ishida, T. Nakajima, Y. Honda, O. Kitao, H. Nakai, T. Vreven, J. A. Montgomery, J. E. Peralta, F. Ogliaro, M. Bearpark, J. J. Heyd, E. Brothers, K. N. Kudin, V. N. Staroverov, R. Kobayashi, J. Normand, K. Raghavachari, A. Rendell, J. C. Burant, S. S. Iyengar, J. Tomasi, M. Cossi, N. Rega, J. M. Millam, M. Klene, J. E. Knox, J. B. Cross, V. Bakken, C. Adamo, J. Jaramillo, R. Gomperts, R. E. Stratmann, O. Yazyev, A. J. Austin, R. Cammi, C. Pomelli, J. W. Ochterski, R. L. Martin, K. Morokuma, V. G. Zakrzewski, G. A. Voth, P. Salvador, J. J. Dannenberg, S. Dapprich, A. D. Daniels, Ö. Farkas, J. B. Foresman, J. V. Ortiz, J. Cioslowski, D. J. Fox, *Gaussian 09, Revision D.01*, Gaussian Inc, Wallingford CT **2009**.
[41] P. Elmer, ChemBioDraw Ultra Version (13.0.0.3015), CambridgeSoft, Waltham, MA (**2012**)
[42] D. Vautherin, D. M. Brink, *Physical Review C.* **1972**, *5*(3), 626.
[43] A. D. Becke, *J. Chem. Phys.* **1993**, *98*(7), 5648.
[44] E. G. Hohenstein, S. T. Chill, C. D. Sherrill, *J. Chem. Theory Comput.* **2008**, *4*(12), 1996.
[45] B. Tüzün, J. Bhawsar, *Arabian Journal of Chemistry* **2021**, *14*(2), 102927.
[46] B. Tüzün, *Turkish Computational and Theoretical Chemistry* **2020**, *4*(2), 76.
[47] D. W. Ritchie, V. Venkatraman, *Bioinformatics (Oxford, England)* **2010**, *26*(19), 2398.
[48] W. DeLano, L. Pymol, *CCP4 Newsletter on Protein Crystallography* **2002**, *40*, 82.
[49] D. Wöhrle, M. Eskes, K. Shigehara, *Synthesis* **1993**, *2*, 194.
[50] G. Venkatesh, M. Govindaraju, C. Kamal, P. Vennilad, S. Kaya, *RSC Adv.* **2017**, *7*, 1401.
[51] X. Ma, Q. Sun, X. Fen, X. He, J. Guo, H. Sun, H. Cao, *Appl. Catal., A* **2013**, *450*, 143.
[52] M. J. Stillman, T. Nyokong, in *Phthalocyanines: Properties and Applications*, (Eds: C. C. Leznoff, A. B. P. Lever) Vol. 1, VCH, New York **1989**.
[53] G.F. Herrmann, F. Shortt, L.A. Sturdy, S.R. Thornton, A. L. Willams, Methods of Organic Chemistry, Vol. E 9 d New York (**1998**) 717–833.
[54] K. Adachi, K. Chayama, H. Watarai, *Langmuir* **2006**, *22*(4), 1630.
[55] E. Kirbaç, A. Erdoğmuş, *J. Mol. Struct.* **2020**, *1202*, 127392.
[56] E. Tokunaga, S. Mori, Y. Sumii, N. Shibat, *ACS Omega* **2018**, *3*, 10912.
[57] A. Ogunsipe, T. Nyokong, *J. Mol. Struct.* **2004**, *689*, 89.
[58] Ç. Çelik, N. Farajzadeh, M. Akın, G. Yaşa Atmaca, Ö. Sağlam, N. Şaki, A. Erdoğmuş, M. Burkut Koçak, *Dalton Trans.* **2021**, *50*, 2736.
[59] A. Phaniendra, D. B. Jestadi, L. Periyasamy, *Indian J. Clin. Biochem.* **2015**, *30*(1), 11.

[60] A. Günsel, E. H. Alici, A. T. Bilgicli, G. Arabaci, M. N. Yarasir, *Turk. J. Chem.* **2019**, *43*, 1030.
[61] J. P. Adjimani, P. Asare, *Toxicol Rep.* **2015**, *2*, 721.
[62] N. Yıldırım, A. T. Bilgiçli, E. H. Alici, G. Arabaci, M. N. Yarasir, *J. Mol. Struct.* **2017**, *1144*, 66e79.
[63] M. S. Ağırtaş, M. E. Güven, S. Gümüş, S. Özdemir, A. Dündar, *Synth. Met.* **2014**, *195*, 177.
[64] N. Farajzadeh, H. Pekbelgin Karaoglu, M. Akin, N. Saki, M. Burkut Kocak, *J. of Porph. And Phthaloc.* **2019**, *23*(1–2), 91.
[65] A. Günsel, A. Kobyaoglu, A. T. Bilgicli, B. Tüzün, B. Tosun, G. Arabaci, M. N. Yarasir, *J. Mol. Struct.* **2020**, *1200*, 127127.
[66] E. H. Alici, A. Gunsel, M. Akin, A. T. Bilgicli, G. Arabaci, M. N. Yarasir, *J. Coordinat. Chem.* **2018**, *71*(19), 3077.
[67] M. Çelebi, M. S. Ağırtas, V. Okumuş, S. Özdemir, *Synth. Met.* **2014**, *195*, 154.
[68] S. Ç. Yavuz, S. Akkoç, B. Tüzün, O. Şahin, E. Saripinar, *Synth. Commun.* **2021**, 1.
[69] A. Aktaş, B. Tüzün, H. A. Taşkın Kafa, K. Sayin, H. Ataseven, *Bratislava Medical Journal-Bratislavske Lekarske Listy* **2020**, *121*(10), 705.
[70] M. A. Gedikli, B. Tuzun, A. Aktas, K. Sayin, H. Ataseven, *Bratislavske Lekarske Listy* **2021**, *122*(2), 101.

SUPPORTING INFORMATION

Additional supporting information may be found online in the Supporting Information section at the end of this article.

How to cite this article: A. T. Bilgiçli, T. Kandemir, B. Tüzün, R. Arıduru, A. Günsel, Ç. Abak, M. N. Yarasir, G. Arabaci, *Appl Organomet Chem* **2021**, *35*(10), e6353. https://doi.org/10.1002/aoc.6353